iScience

CellPress
OPEN ACCESS

Article

Prdm12 represses the expression of the visceral neuron determinants Phox2a/b in developing somatosensory ganglia

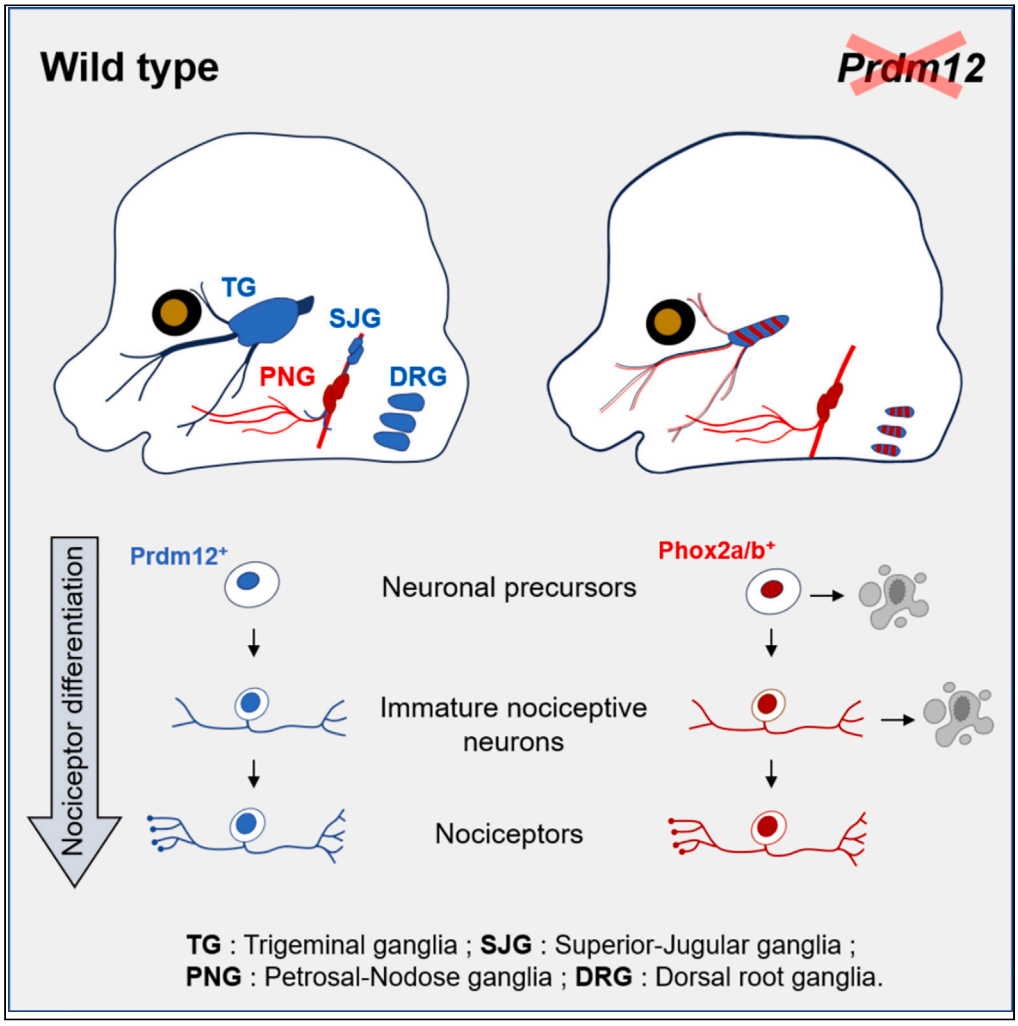

Simon Vermeiren, Pauline Cabochette, Maya Dannawi, ..., Benoit Vanhollebeke, Jean-François Brunet, Eric J. Bellefroid

ebellefr@ulb.ac.be

Highlights

Loss of Prdm12 induces Bax-dependent apoptosis in developing somatosensory ganglia

Prdm12 represses the visceral determinants Phox2a/b in somatosensory ganglia

Repression of Phox2a/b by Prdm12 is time and context dependent

Visceral fate switch of surviving ectopic Phox2a/b cell is incomplete

Vermeiren et al., iScience 26, 108364
December 15, 2023
https://doi.org/10.1016/j.isci.2023.108364

iScience

CellPress
OPEN ACCESS

Article

Prdm12 represses the expression of the visceral neuron determinants Phox2a/b in developing somatosensory ganglia

Simon Vermeiren,[1] Pauline Cabochette,[1,7] Maya Dannawi,[1,7] Simon Desiderio,[1,7] Alba Sabaté San José,[1] Younes Achouri,[2] Sadia Kricha,[1] Maren Sitte,[3] Gabriela Salinas-Riester,[3] Benoit Vanhollebeke,[1] Jean-François Brunet,[4,5,6] and Eric J. Bellefroid[1,8,*]

SUMMARY

Prdm12 is a transcriptional regulator essential for the emergence of the somatic nociceptive lineage during sensory neurogenesis. The exact mechanisms by which Prdm12 promotes nociceptor development remain, however, poorly understood. Here, we report that the trigeminal and dorsal root ganglia hypoplasia induced by the loss of *Prdm12* involves Bax-dependent apoptosis and that it is accompanied by the ectopic expression of the visceral sensory neuron determinants *Phox2a* and *Phox2b*, which is, however, not sufficient to impose a complete fate switch in surviving somatosensory neurons. Mechanistically, our data reveal that Prdm12 is required from somatosensory neural precursors to early post-mitotic differentiating nociceptive neurons to repress *Phox2a/b* and that its repressive function is context dependent. Together, these findings reveal that besides its essential role in nociceptor survival during development, Prdm12 also promotes nociceptor fate via an additional mechanism, by preventing precursors from engaging into an alternate Phox2 driven visceral neuronal type differentiation program.

INTRODUCTION

The vertebrate nervous system is deeply divided into "somatic" and "visceral" subsystems. In the sensory pathways, somatic neurons project to the skin but also to muscles, joints, and viscera. They detect sensations that organisms "feels" (all sensations that are conscious such as pressure, light touch, muscle extension, joint position, heat, cold, itch, and pain). Visceral sensory neurons (VSN) respond to internal stimuli and control often in an unconscious way the activity of several body's systems (respiratory, digestive, cardiovascular …) to assure homeostasis.[1–3] In the trunk, somatosensory neurons (SSN) are located in the dorsal root ganglia (DRG). In the head, they are located in the trigeminal ganglia (TG) and in the proximal ganglia of nerves VII, IX, and X (i.e., the proximal part of the geniculate ganglia [GG] and the superior and jugular ganglia [SJG]) and the special somatosensory vestibulocochlear ganglia (VG). VSN form the distal part of the GG,[4] and the petrosal and nodose (PNG) ganglia (distal ganglia associated with cranial nerves IX and X). During peripheral nervous system (PNS) development, those ganglia arise from distinct embryonic populations. While DRG and proximal GG/SJG derive exclusively from neural crest (NC) cells, distal GG and PNG develop from distinct epibranchial placodes, and VG from the otic placode, with a possible minor contribution of NC. TG are in contrast of mixed origin.[5] How this somatic/visceral dichotomy is established in developing sensory neurons remains largely unknown. One transcription factor, however, stands out in this process, the evolutionarily conserved homeoprotein Phox2b that, together with its close relative Phox2a, act as determinants of visceral neuronal fate in both afferent pathways (as well as their targets in the hindbrain) and efferent autonomic pathways.[4,6–10] In sensory pathways, no counterpart regulator of the somatic neuronal fate has yet been identified.

The *Prdm12* gene encodes an evolutionarily conserved zinc finger transcriptional regulator selectively expressed in nociceptors, the SSN specialized to detect noxious stimuli and in C-low-threshold mechanosensitive neurons (C-LTMRs) that become activated in response to light mechanical stimulation.[11–13] Inactivation of Prdm12 leads to a marked hypoplasia of TG, DRG, and SJG, due to a selective loss of nociceptive and C-LTMRs, while the other subtypes of sensory neurons, the myelinated mechanoreceptors (LTMRs) and proprioceptors are

[1]Department of Molecular Biology, ULB Neuroscience Institute (UNI), Université libre de Bruxelles (ULB), B-6041 Gosselies, Belgium
[2]Transgenesis Platform, de Duve Institute, Université Catholique de Louvain, Institut de Duve, Brussels, Belgium
[3]NGS Integrative Genomics, Department of Human Genetics at the University Medical Center Göttingen (UMG), 37075 Göttingen, Germany
[4]Institut de Biologie de l'ENS (IBENS), Inserm, CNRS, École Normale Supérieure, PSL Research University, 75005 Paris, France
[5]Centre National de la Recherche Scientifique, Unité Mixte de Recherche 8197, 75005 Paris, France
[6]Institut National de la Santé et de la Recherche Médicale U1024, 75005 Paris, France
[7]These authors contributed equally
[8]Lead contact
*Correspondence: ebellefr@ulb.ac.be
https://doi.org/10.1016/j.isci.2023.108364

unaffected.[11–13] This observation explains why human patients with homozygous mutations in *PRDM12* gene are unable to feel pain from birth.[14] The exact mechanisms by which Prdm12 promotes nociceptor development remain, however, poorly understood. Here, we investigate these mechanisms, with an initial focus on developing cranial sensory ganglia in which Prdm12 function and mode of action have not been characterized yet. Our results reveal that, besides promoting survival of developing TG and DRG nociceptors, Prdm12 is also essential to prevent them to embark into an alternate visceral neuronal fate program.

RESULTS

Prdm12 is expressed independently of Neurog1 in cranial somatosensory ganglia

To study the role of Prdm12 in cranial sensory ganglia, we first reevaluated its expression during their development. Figure S1 shows that, as previously reported,[11] Prdm12 is detected in developing nociceptors in TG, DRG, and SJG. We found that it is also expressed in the developing VAG but not in the somatic part of the GG, containing only mechanoreceptors, and is absent in epibranchial ganglia (GG, PNG) containing VSN. Unlike in DRG, Prdm12 temporal expression profile has not yet been investigated in TG and SJG. Therefore, we performed double immunostainings on mouse head sections at different embryonic stages, comparing Prdm12 expression to that of the NC cell marker Sox10 and the pan-neuronal marker Islet1.[15,16] We observed that at E10.5, Prdm12 is almost exclusively expressed in Sox10$^+$ cells in both ganglia (Figure 1A). In TG, performing phospho-histone H3 (H3P$^+$) stainings which marks proliferating cells in late G2 and M phase (thereby labeling only a fraction of the cycling cells), we found that at E10.5, only some rare Prdm12$^+$ cells are H3P$^+$ cells, suggesting that most Prdm12$^+$Sox10$^+$ cells are already postmitotic (Figure 1B). From E11.5 onwards, Prdm12 becomes progressively excluded from Sox10$^+$ cells and increasingly co-expressed with Islet1 (Figure 1C). Thus, as observed in DRG, Prdm12 appears to be expressed from NC sensory precursors during the development of cranial SSN.

In DRG, neurogenesis occurs in two temporal overlapping waves controlled by the proneural genes *Neurog2* and *Neurog1*, *Neurog1* being activated during the second wave of neurogenesis which generates most of the nociceptors. In TG and SJG, however, neurogenesis is almost exclusively under *Neurog1* control.[17–19] Previous studies have shown that in DRG *Prdm12* is expressed in both Neurog2$^+$ and Neurog1$^+$ precursors and that in the absence of *Neurog1*, Prdm12$^+$ nociceptors are dramatically reduced in number.[11,12] To determine how *Prdm12* expression is related to that of *Neurog1* during cranial sensory neurogenesis and define the onset of their respective activation, we compared their expression in TG and SJG of E11.5 and E12.5 *Neurog1*$^{GFP/+}$ mouse embryos.[18] At E11.5, in both cranial ganglia, we observed that most GFP$^+$ cells do not co-express Prdm12 and that conversely, the majority of Prdm12$^+$ cells are GFP$^-$, while at E12.5 the vast majority of GFP$^+$ cells now co-express Prdm12, as observed in DRG (Figure 1D). So, it appears there are at that stage two populations of cells that transition from mutually exclusive expression of one of the gene, to co-expression. While in TG and DRG some of the GFP$^+$Prdm12$^-$ cells may correspond to cells of the first wave of neurogenesis giving rise to the mechanoreceptor lineage, this is not the case in SJG that are exclusively constituted of Prdm12$^+$ neurons and do not contain mechanoreceptors. We then assessed whether Prdm12 expression in cranial ganglia is affected by the loss of *Neurog1*, which has been reported to severely compromise neurogenesis in TG and SJG.[18,19] Despite the absence of neurons at TG and SJG prospective position in *Neurog1*$^{GFP/GFP}$ knockout embryos, Prdm12$^+$ cells could still be observed at the levels of their respective nerves (Figure 1E). Thus, Prdm12 activation occurs independently of neurogenins in both cranial and trunk ganglia.

Prdm12 depletion causes TG and DRG hypoplasia partly through Bax-dependent apoptosis

To assess the consequences of Prdm12 loss in cranial ganglia of *Prdm12*$^{LacZ/LacZ}$ embryos, we performed Islet1 immunostaining in a *Sox10*-Venus reporter background.[20] Using this system, we confirmed the previously reported hypoplasia of the TG and agenesis of SJG in E11.5 *Prdm12*$^{LacZ/LacZ}$ embryos[11] (Figure 2A). Despite the reduced number of generated neurons and the absent expression of *Ntrk1*, encoding the tyrosine kinase receptor TrkA that is required for nociceptive neuron survival, we found that *Neurog1* and other downstream proneural factors such as *NeuroD1* were, however, detected in the hypoplastic TG of *Prdm12*$^{LacZ/LacZ}$ embryos, indicating that neurogenesis is not compromised *per se* (Figure 2B).

The mechanism by which the loss of *Prdm12* induces hypoplasia of cranial somatosensory ganglia remains unclear.[11–13] Therefore, we looked at potential cell proliferation and survival defects in TG of *Prdm12*$^{LacZ/LacZ}$ embryos at E10.5 before the onset of *Ntrk1* activation. We found that the total number of cells as well as the number of Sox10$^+$ NC progenitors co-expressing activated-Caspase3 is increased in TG of *Prdm12*$^{LacZ/LacZ}$ embryos compared to controls (Figure 2C). In contrast, the overall number of proliferative cells evaluated using H3P staining, and the number of proliferative Sox10$^+$ NC progenitors evaluated using H3P and Sox10 co-staining was similar in TG of *Prdm12*$^{LacZ/LacZ}$ and control embryos (Figure 2D). To further investigate the role of Prdm12 in the survival of nociceptive neurons, we next examined in TG, SJG, and DRG the effect of the loss of *Prdm12* in a proapoptotic *BCL-2 homolog Bax*$^{-/-}$ background known to prevent neuronal death that takes place in the absence of NGF or TrkA.[21,22] In TG and DRG, we found that the number of neurons (detected using Islet1 or Tlx3 immunostaining) in E13.5 *Prdm12*$^{LacZ/LacZ}$; *Bax*$^{-/-}$ embryos is increased compared to that of *Prdm12*$^{LacZ/LacZ}$ embryos (Figure 3A). On the opposite, no rescue of SJG development was observed in E13.5 *Prdm12*$^{LacZ/LacZ}$; *Bax*$^{-/-}$ indicating that the observed agenesis of SJG is not dependent of Bax-mediated apoptosis (Figure 3B). Importantly, no TrkA$^+$ neurons could be observed in TG and DRG of *Prdm12*$^{LacZ/LacZ}$; *Bax*$^{-/-}$ embryos, indicating that loss of TrkA expression is a direct effect of *Prdm12* ablation, rather than a secondary consequence of cell death. The fact that the deletion of Bax only partially rescues TG and DRG development and does not rescue at all SJG development suggests that Prdm12 also contributes to sensory ganglia formation via other mechanisms.

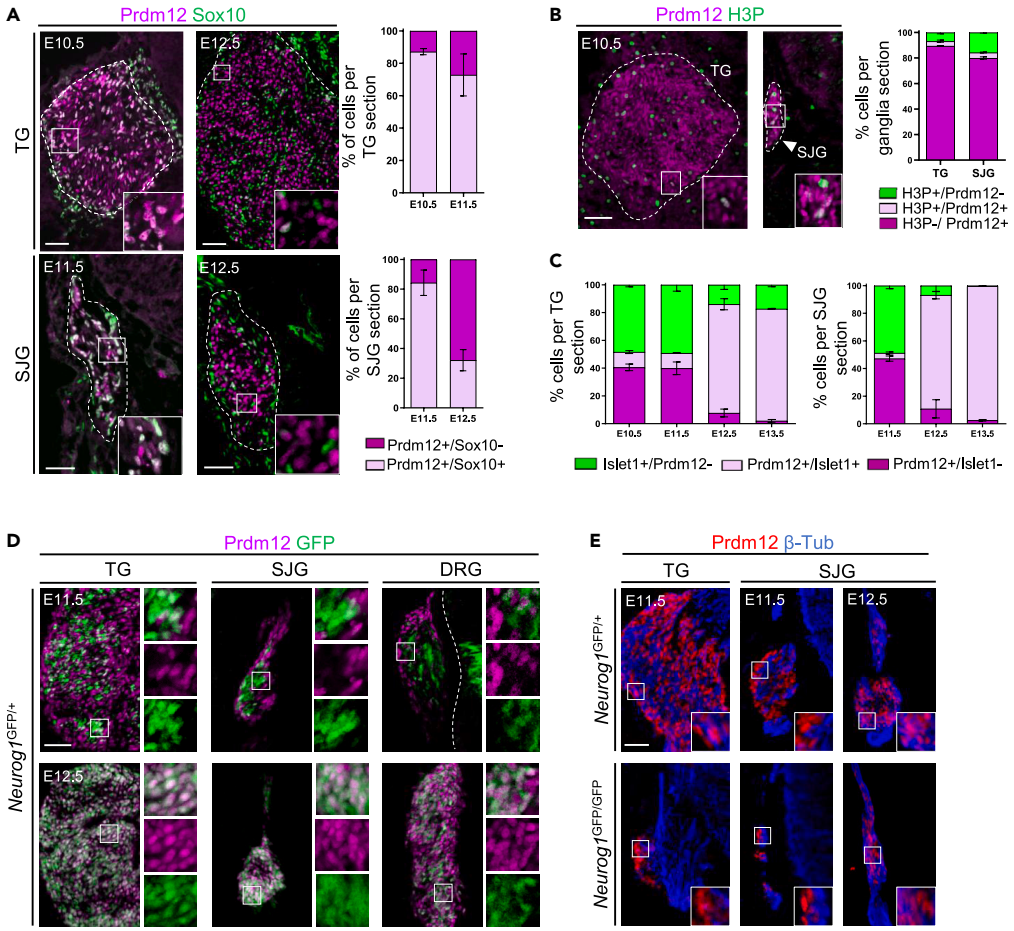

Figure 1. Prdm12 is expressed from neural crest precursors in developing cranial somatosensory ganglia independently of Neurog1

(A) Immunostaining for Prdm12 and the neural crest cell marker Sox10 on coronal sections through TG and SJG of mouse embryos at indicated stages. The proportion of Prdm12^{+} cells expressing Sox10 or not is represented in the histogram.

(B) Immunostaining with Prdm12 and H3P antibodies on coronal sections through TG and SJG of E10.5 mouse embryos. Graph on the right show quantification of the immunostainings. In A and B, the ganglia are delimitated with a dashed line and insets show high magnification of double labeled cells.

(C) Quantifications of cells positive for Prdm12 and/or the post-mitotic sensory neuron marker Islet1 detected on coronal sections through mouse TG or SJG at the indicated embryonic stages.

(D) Immunostaining with Prdm12 and GFP antibodies on coronal sections through TG, SJG, and DRG of *Neurog1*$^{GFP/+}$ mouse embryos at E11.5 and E12.5. Insets show magnification of region with representative Prdm12 staining.

(E) Images of mixed and individual channels are represented (E) Immunostaining with Prdm12 and β-Tubulin antibodies on coronal sections through TG and SJG of *Neurog1*$^{GFP/+}$ and *Neurog1*$^{GFP/GFP}$ mouse embryos at E11.5 and E12.5. Insets show magnification of region with representative Prdm12 staining. Scale bars, 50 μm. SJG, superior-jugular ganglia; TG, trigeminal ganglia; DRG, dorsal root ganglia.

Loss of Prdm12 upregulates in trigeminal ganglia the expression of markers enriched in nodose ganglia neurons

Although the previous data indicate that most developing somatosensory nociceptive neurons lacking Prdm12 die during neurogenesis, many X-Gal-stained cells can still be detected in TG and DRG of *Prdm12*$^{LacZ/LacZ}$ embryos at E13.5 and E14.5[11] (Figure 4A), suggesting that some of them survive until at least those stages without expressing it. We speculated that these cells that have lost *Prdm12* may survive because they adopt an alternate fate. To test this hypothesis, we analyzed by bulk RNA-seq the transcriptome of dissected TG of E13.5 *Prdm12*$^{LacZ/LacZ}$ and control embryos. Using an adjusted p value $\leq$0,05 and an absolute Log2 fold change (FC) of $\geq$1, a list of 341 differentially expressed genes (DEGs) was obtained, among which 180 were up and 161 downregulated (Figure S2A and Table S1). As expected, nociceptive neuronal markers such as *Ntrk1*, *Scn10a*, *Trpv1*, *Runx1*, or *Ret*, and markers of C-LTMRs (also expressing Prdm12) such as *TH* were among the most downregulated. The downregulation of some of them was validated by ISH/IF (Figures S2B and S2C). The purinergic receptor P2X2 (*P2rx2*) and the zinc finger transcription factor Gata3 which are minimally expressed in adult DRG neuron classes[23] were among the most upregulated genes. Figure 4B shows that they are indeed upregulated by the loss of Prdm12. Among the list of upregulated DEG was also the brain-derived neurotrophic factor (BDNF)-receptor TrkB (*Ntrk2*) that in TG and DRG is selectively expressed in Prdm12 negative large

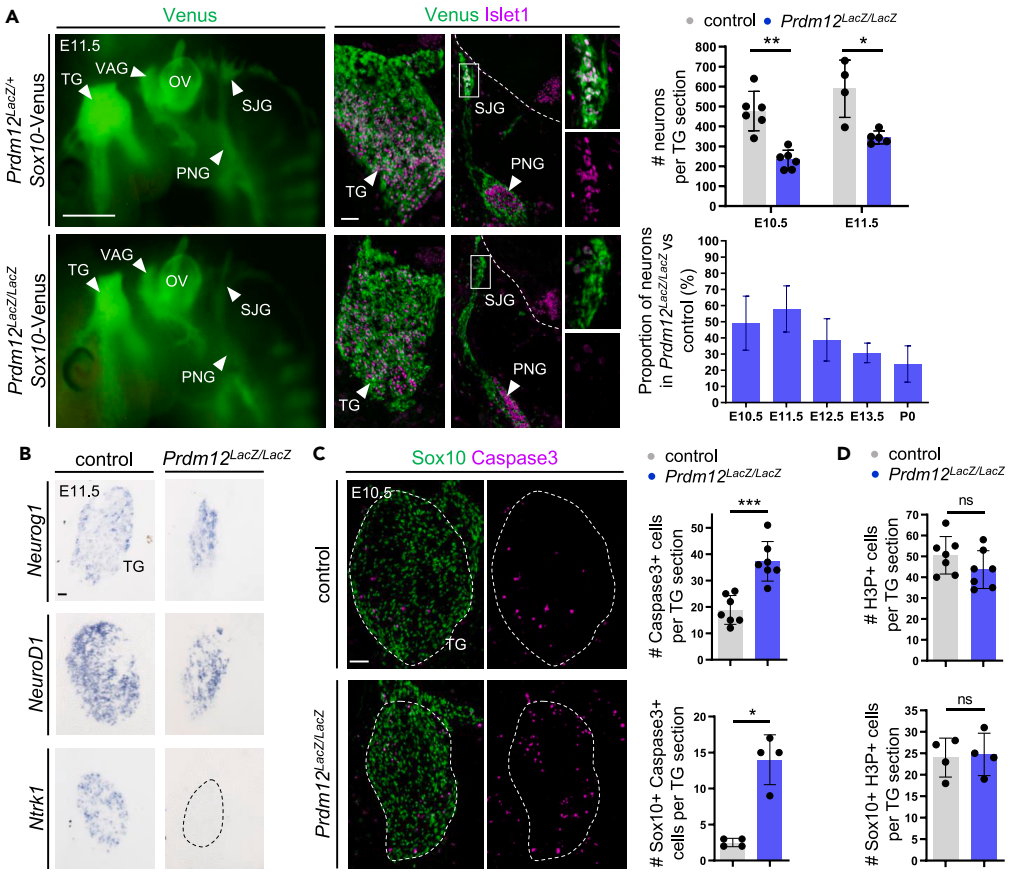

Figure 2. Loss of Prdm12 causes trigeminal and dorsal root ganglia hypoplasia partly through neural crest precursor apoptosis

(A) Lateral views of the head of E11.5 *Sox10*-Venus *Prdm12*$^{LacZ/+}$ control and *Sox10*-Venus *Prdm12*$^{LacZ/LacZ}$ mouse embryos showing TG hypoplasia and agenesis of the SJG in *Prdm12*$^{LacZ/LacZ}$ embryos (scale bar, 1000 μm). Right panels show immunostainings with the pan-neuronal marker Islet1 on coronal sections through TG, SJG, and PNG of E11.5 control and *Prdm12*$^{LacZ/LacZ}$ embryos expressing the *Sox10*-Venus reporter cassette. Insets show Venus with Islet1 and Islet1 staining alone of the indicated area showing the near complete loss of Islet1^{+} neurons in *Prdm12*$^{LacZ/LacZ}$ SJG (scale bars, 50 μm). Graphs show the quantification of the number of neurons (Islet1^{+} or Tlx3^{+} cells) in TG of *Prdm12*$^{LacZ/LacZ}$ and control embryos at indicated stages. Absolute and relative numbers, in comparison to the controls, are shown.

(B) *In situ* hybridization with *Neurog1*, *NeuroD1*, and *Ntrk1* antisense probes on coronal sections through TG of E11.5 control and *Prdm12*$^{LacZ/LacZ}$ embryos.

(C) Immunostainings using antibodies for Sox10 and cleaved-Caspase3 on coronal sections through TG of control and *Prdm12*$^{LacZ/LacZ}$ embryos at E10.5 with quantifications showing increased number of apoptotic cells and apoptotic Sox10^{+} progenitors in TG anlagen of *Prdm12*$^{LacZ/LacZ}$ embryos.

(D) Quantifications obtained from immunostainings using antibodies for Sox10 and H3P on coronal sections through TG of E10.5 control and *Prdm12*$^{LacZ/LacZ}$ embryos showing that the number of H3P^{+} cells and of H3P^{+} Sox10^{+} progenitors is not affected. Histograms are represented as mean ± standard deviation (SD). Each dot in histograms represents the mean values obtained for an individual biological replicate. Mann-Whitney tests have been applied. Calculated p values are referred to as follow: *p < 0,05; **p < 0,01; ***p < 0.001 and ns for non-significant difference (p > 0,05). Scale bars in B and C, 50 μm. DRG, dorsal root ganglia; OV, otic vesicle; PNG, petrosal-nodose ganglia; SJG, superior-jugular ganglia; TG, trigeminal ganglia; VAG, vestibuloacoustic ganglia.

diameter LTMR. Figure 4C shows that an increased number of TrkB^{+} neurons was observed in *Prdm12*$^{LacZ/LacZ}$ TG while *Ntrk3*/TrkC, another recognized LTMR marker[23] was in contrast not misregulated. Measurements of neuron soma areas showed a shift in the proportion of small diameter cells expressing TrkB, suggesting its ectopic expression in putative nociceptive precursors in *Prdm12*$^{LacZ/LacZ}$ TG (Figure 4D). We then cross-referenced our list of DEGs to recently established single-cell RNA sequencing-based DRG neuron subtype classifications.[23,24] While as expected downregulated DEGs were enriched in nociceptive neuronal gene classes versus LTMR/proprioceptive classes (31 ± 8 versus 15 ± 4; mean number of gene per class ±SD), upregulated genes did not show a significant enrichment in nociceptive versus non-nociceptive DRG neuronal gene classes (13 ± 5 vs. 11 ± 4; mean ± SD) (Figure S2D, Table S2). These results suggest that in TG, surviving precursors lacking Prdm12 adopt an alternate neuronal fate that does not correspond to any other DRG SSN classes.

As one of the most upregulated genes in our list, *Tmc3*, encoding a putative mechanosensory channel has been reported to be expressed in nodose ganglia VSN,[25] we next cross-referenced our list of DEGs to the adult vagal nerve ganglia neuron gene expression atlas.[26] While no particular enrichment was attributed to downregulated genes (mean number of genes per jugular ganglia (JG) versus nodose ganglia (NG) neuron classes of 26 ± 4 versus 20 ± 3; mean ± SD), we found that the upregulated DEGs are more enriched in NG neuronal

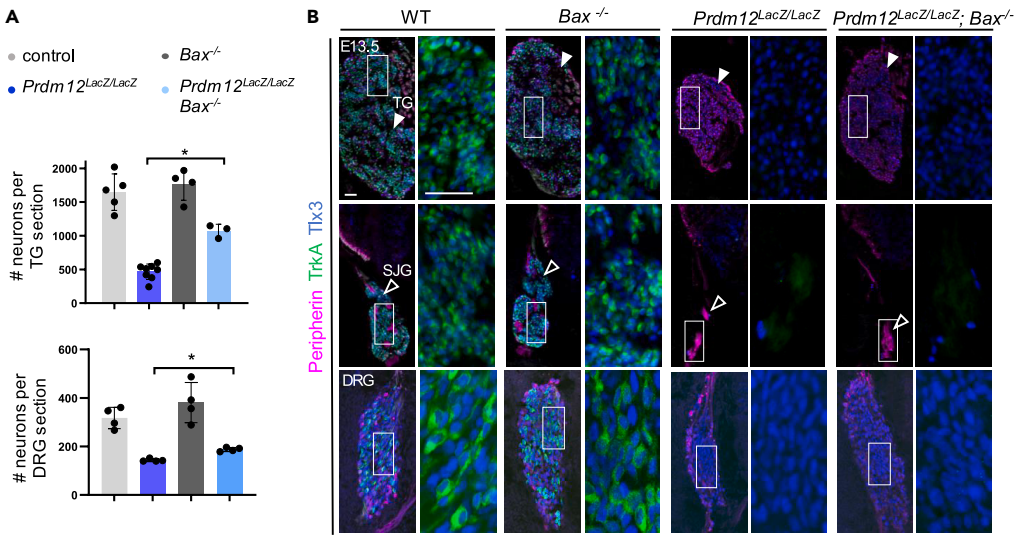

Figure 3. Inhibition of Bax-dependent apoptosis partly rescues trigeminal and dorsal root ganglia hypoplasia caused by the loss of Prdm12 but does not restore TrkA expression

(A) Graphs showing the number of neurons (detected by immunostaining with Islet1 or Tlx3 antibody) in TG or DRG coronal sections of E13.5 embryos of indicated genotypes.

(B) Immunostainings using Peripherin, TrkA and Tlx3 antibodies on coronal sections through TG, SJG, and DRG of E13.5 control, *Prdm12*$^{LacZ/LacZ}$, *Bax*$^{-/-}$ and *Prdm12*$^{LacZ/LacZ}$; *Bax*$^{-/-}$ embryos. Scale bar, 50 μm. Histograms are represented as mean ± standard deviation (SD). Each dot in histograms represents the mean value obtained for an individual biological replicate. Mann-Whitney tests have been applied. Calculated p values are referred to as follow: *p < 0,05; **p < 0,01; ***p < 0.001 and ns for non-significant difference (p > 0,05). DRG, dorsal root ganglia; SJG, superior-jugular ganglia; TG, trigeminal ganglia.

classes than in JG classes (16 ± 3 versus 7 ± 2 genes per class; mean ± SD) (Figure S2E, Table S3). Among the upregulated DEGs enriched in NG neuronal classes was the transcription factor *Phox2a* that is among the most defining genes for placode derived nodose neurons but that is also expressed in sympathetic and enteric neurons[24,26] (Figure S2A). Therefore, double immunostainings were performed with Phox2a and Islet1 or Tlx3 antibodies on TG of *Prdm12*$^{LacZ/LacZ}$ embryos between E12.5 and P0. Results obtained indicate that Phox2a$^+$ cells are found in about 30% of all TG neurons at E12.5 and that their number progressively decreases with time. While at E12.5 some of these Phox2a$^+$ cells were not co-expressing Islet1 or Tlx3 and thus likely correspond to Phox2a$^+$ progenitors, later on all of them express it and thus represent post-mitotic Phox2a$^+$ ectopic neurons (Figure 4E). Subclassification of upregulated DEGs into genes expressed only in Prdm12$^+$ ganglia (i.e., JG and/or DRG) or only in Phox2$^+$ ganglia (i.e., NG, SG, and/or ENS) revealed an enrichment of upregulated DEGs in Phox2$^+$ PNS structures, with 21 on 33 of these genes being NG markers (Figure S2F, Tables S4 and S5). We examined the expression of some of these DEGs (*P2rx2* and *Ntrk2*) with enriched expression in NG neuron classes and found that, like Phox2a/b, they are expressed in developing PNG (Figure S2G and Table S4). Thus, precursors lacking *Prdm12* that survive in TG appear to initiate a Phox2a driven differentiation program to acquire an NG VSN-like fate. To test this hypothesis, as *Ntrk2*/TrkB marks VSN in PNG but also populations of LTMR neurons in which Prdm12 is virtually not expressed,[11] we asked whether some of the TrkB$^+$ supernumerary neurons found in *Prdm12*$^{LacZ/LacZ}$ TG co-express the NG neuron marker Phox2a. Phox2a expression was indeed observed selectively in TG of E13.5 *Prdm12*$^{LacZ/LacZ}$ embryos and 69,2% ± 4,8% (mean ± SD) of these Phox2a expressing cells co-expressed TrkB, indicating that supernumerary TrkB$^+$ neurons could represent cells aberrantly engaged to acquire characteristics of NG VSN (Figure 4F). Consistently, Phox2a$^+$ neurons co-expressing Gata3 were also detected in TG of E13.5 *Prdm12*$^{LacZ/LacZ}$ embryos by double immunostaining (Figure 4G). Those Phox2a$^+$/Gata3$^+$ neurons represent only a fraction of the Phox2a$^+$ ectopic neurons (33,9% ± 3,1%; mean ± SD), which may reflect the more restricted expression of Gata3 than that of Phox2a in NG neuron subtypes.[26]

Loss of *Prdm12* transiently upregulates Phox2b in neural crest derived cells of developing trigeminal and dorsal root ganglia

Phox2a expression precedes and positively regulates Phox2b in cranial viscerosensory ganglia.[27] As Phox2b has a predominant function over Phox2a[9] but was just below the cut-off used in our list of upregulated DEG (FC of 0,92), we examined its expression *Prdm12*$^{LacZ/LacZ}$ embryos. By immunostaining, we found that Phox2b, like Phox2a, is ectopically expressed in TG of *Prdm12*$^{LacZ/LacZ}$ embryos. While only very few Phox2b$^+$ cells are already detectable in TG of E10.5 *Prdm12*$^{LacZ/LacZ}$ embryos (data not shown), they represent about 40% of the neurons at stages E12.5 and E13.5. As observed for Phox2a, this number decreases later on, suggesting that many of those ectopic Phox2b$^+$ cells are eliminated with time (Figure 5A). To test this idea, we compared the number of Phox2b$^+$ neurons in TG and DRG of *Prdm12*$^{LacZ/LacZ}$ and *Prdm12*$^{LacZ/LacZ}$; *Bax*$^{-/-}$ E13.5 embryos. An increase in the number of Phox2b$^+$ neurons was observed in both TG and DRG following

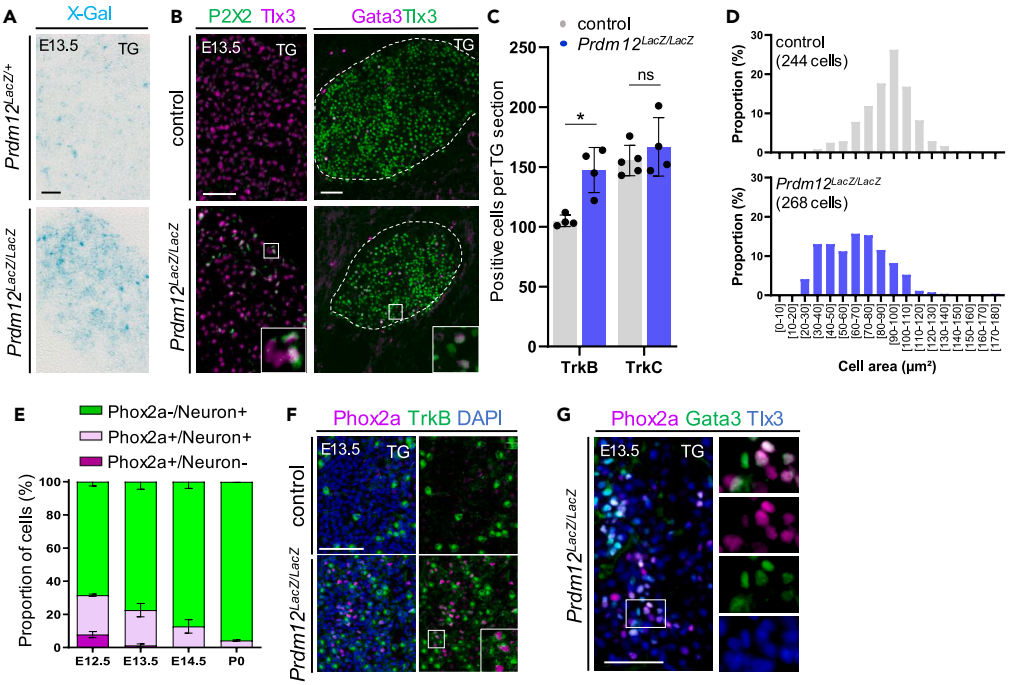

Figure 4. Loss of Prdm12 leads to ectopic expression of visceral sensory neuron markers in developing trigeminal ganglia

(A) X-Gal staining on coronal sections through TG of E13.5 *Prdm12*$^{LacZ/+}$ and *Prdm12*$^{LacZ/LacZ}$ embryos showing that many cells that should have expressed *Prdm12* are still present in knock-out embryos.

(B) Immunostainings of P2X2 with Tlx3 and Gata3 with Tlx3 on coronal sections through TG of E13.5 *Prdm12*$^{LacZ/LacZ}$ and control embryos. Note the ectopic expression of P2X2 and Gata3 in Tlx3$^+$ neurons.

(C) Graphs showing the number of TrkB or TrkC-expressing cells in TG coronal sections compared between E13.5 control and *Prdm12*$^{LacZ/LacZ}$ embryos.

(D) Histograms representing the percentage of TrkB-expressing cells of indicated range of soma area observed in TG sections of E13.5 control and *Prdm12*$^{LacZ/LacZ}$ embryos.

(E) Quantification of Phox2a$^+$ neurons and progenitors in TG of *Prdm12*$^{LacZ/LacZ}$ embryos at indicated stages as revealed by co-immunostainings for Islet1 or Tlx3 used as postmitotic neuronal markers.

(F) Immunostainings of Phox2a and TrkB on TG sections of E13.5 control and *Prdm12*$^{LacZ/LacZ}$ embryos counterstained with DAPI.

(G) Immunostaining revealing Phox2a$^+$/Gata3$^+$/Tlx3$^+$ neurons in coronal sections through E13.5 TG of *Prdm12*$^{LacZ/LacZ}$ embryos. Insets show high magnifications of the individual immunostainings of the indicated area. Histograms are represented as mean ± standard deviation (SD). Each dot in histograms represents the mean values obtained for an individual biological replicate. Mann-Whitney tests have been applied. Calculated p values are referred to as follow: *p < 0,05; **p < 0,01; ***p < 0.001 and ns for non-significant difference (p > 0,05). Scale bars, 50 µm. TG, trigeminal ganglia.

inhibition of programmed cell death, suggesting that some ectopic Phox2b$^+$ neurons may indeed be cleared out with time by Bax-dependent apoptosis (Figure 5B).

Phox2b is expressed in the PNS in all autonomic ganglia, in epibranchial placode derived ganglia and in some CNS structures.[6–10] To assess the cellular origin of these ectopic Phox2b$^+$ neurons in *Prdm12*$^{LacZ/LacZ}$ TG, we first compared Phox2b expression to that of the β-Galactosidase (β-Gal). As expected, the vast majority of ectopic Phox2b$^+$ cells are β-Gal$^+$ in TG of *Prdm12*$^{LacZ/LacZ}$ embryos. However, not all β-Gal$^+$ cells were Phox2b$^+$, suggesting that the loss of Prdm12 either only lead to a VSN NG-like fate acquisition in a subgroup of neural precursors or that Phox2b gene activation is transient (Figure 5C). Double immunostainings with Phox2b and Sox10 antibodies were then performed on sections through TG of E11.5 *Prdm12*$^{LacZ/LacZ}$ embryos showing that some ectopic Phox2b$^+$ cells express Sox10. In TG of E11.5 *Prdm12*$^{LacZ/LacZ}$ embryos with a *Sox10*-Venus background, we also found that most Phox2b$^+$ cells are also Venus$^+$ suggesting that many of these ectopic Phox2b$^+$ cells are of NC origin (Figure S3A). At that stage we also noticed an increased number of Phox2b$^+$ cells along the trigeminal nerve (nV) of *Prdm12*$^{LacZ/LacZ}$ embryos compared to controls. These Phox2b$^+$ cells do not express Sox10 or Tlx3 and thus do not correspond to NC cells or ectopic TG neurons. We speculated that these ectopic Phox2b$^+$ cells may be CNS cells that accumulate along the TG nerves of *Prdm12*$^{LacZ/LacZ}$ embryos. Supporting this hypothesis, we found that the hindbrain trigeminal nuclei marker Nkx6.1,[8,28,29] one the most highly upregulated gene in our DEG list, was detected in those Phox2b$^+$Tlx3$^-$ cells (Figure S3B). To determine the extent of Phox2b activation in TG of *Prdm12*$^{LacZ/LacZ}$ embryos, we turned to the *Phox2b*$^{Cre/+}$; *Rosa26*$^{LSL\text{-}tdTomato/+}$ reporter system that allows persistent expression of tdTomato in cells that have activated *Phox2b*.[4] We observed massive tdTomato signal in TG but also in DRG neurons and nerve fibers of *Prdm12*$^{LacZ/LacZ}$ embryos compared to controls (Figures 5D and 5E). In the TG of *Prdm12*$^{LacZ/LacZ}$ embryos, we found that 34,4 ± 2,3% of the

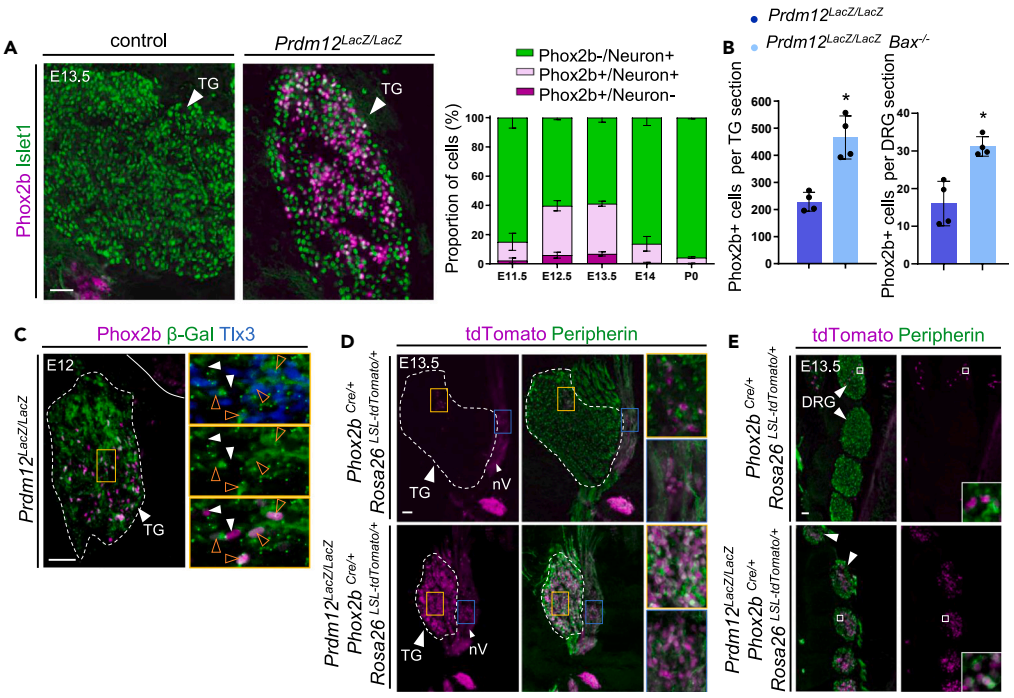

Figure 5. Loss of Prdm12 leads to transient ectopic activation of Phox2b in trigeminal and dorsal root ganglia

(A) Left, immunostaining using an antibody for Phox2b and the pan-sensory neuron marker Islet1 on a coronal section through the TG of E13.5 *Prdm12*$^{LacZ/LacZ}$ and control embryos, showing the presence of ectopic Phox2b^{+} cells in TG of knock-out embryos. Right, the graph shows the proportion of Phox2b^{+} neurons and progenitors as revealed by immunostaining with the neuronal markers Islet1 or Tlx3 in TG of *Prdm12*$^{LacZ/LacZ}$ embryos at the indicated stages.

(B) Quantification of Phox2b^{+} neurons in TG and DRG of E13.5 *Prdm12*$^{LacZ/LacZ}$; *Bax*$^{-/-}$ and *Prdm12*$^{LacZ/LacZ}$ embryos revealing their increased number in *Prdm12*$^{LacZ/LacZ}$; *Bax*$^{-/-}$ embryos.

(C) Triple immunostaining with Phox2b, β-Galactosidase (β-Gal) and Tlx3 antibodies on coronal sections through TG of E12 *Prdm12*$^{LacZ/LacZ}$ embryos. Insets show high magnifications of the indicated area with β-Gal channel alone and channel combinations for β-Gal and Phox2b or for β-Gal and Tlx3 showing that most Phox2b^{+} Tlx3^{+} neurons (pointed by orange empty arrowheads) are β-Gal^{+}. White arrowheads point to some rare Phox2b^{+} Tlx3^{+} β-Gal^{-} cells.

(D) Immunostainings using antibodies for Peripherin and tdTomato performed on coronal sections through TG of *Prdm12*$^{LacZ/LacZ}$ and control P0 pups in a *Phox2b*$^{Cre/+}$; *Rosa26*$^{LSL\text{-}tdTomato/+}$ background. Orange and blue framed insets are high magnifications of the indicated area in TG and trigeminal nerve (nV), respectively, showing that a large increase of ectopic tdTomato^{+} neurons is detected in TG of *Prdm12*$^{LacZ/LacZ}$ compared to controls.

(E) Horizontal sections through cervical DRG of E13.5 *Prdm12*$^{LacZ/LacZ}$; *Phox2b*$^{Cre/+}$; *Rosa26*$^{LSL\text{-}tdTomato/+}$ and control embryos immunostained with tdTomato and Peripherin antibodies. Histograms are represented as mean ± standard deviation (SD). Each dot in histograms represents the mean values obtained for an individual biological replicate. Mann-Whitney tests have been applied. Calculated p values are referred to as follow: *p < 0,05; **p < 0,01; ***p < 0.001 and ns for non-significant difference (p > 0,05). Scale bars, 50 μm. DRG, dorsal root ganglia; TG, trigeminal ganglia.

neurons were Phox2b^{+} at E13,5 and 4,1 ± 0,7% at P0, while 56,5 ± 3,8% of the neurons were dTom^{+} at E13.5 and 37,2 ± 4,9% at P0. Thus, in *Prdm12*$^{LacZ/LacZ}$ embryos, *Phox2b* is transiently ectopically expressed in TG and in DRG.

Ectopic expression of Phox2b does not change the innervation pattern of trigeminal neurons

To examine the fate of ectopic Phox2b^{+} cells in *Prdm12*$^{LacZ/LacZ}$ embryos, we followed tdTomato^{+} neurons in somatosensory ganglia of *Prdm12*$^{LacZ/LacZ}$; *Phox2b*$^{Cre/+}$; *Rosa26*$^{LSL\text{-}tdTomato/+}$ embryos. In TG, we found that they express VSN markers Gata3 and TrkB, but still retain expression of the pan-SSN marker Brn3a, arguing for a mixed neuronal identity (Figures S4A and S4B). While only some ectopic Phox2a/b^{+} neurons seemed to survive until birth in TG of *Prdm12*$^{LacZ/LacZ}$ newborns (representing 4,1 ± 0,7% of total neurons per section; mean ± SD), still an important number of tdTomato^{+} neurons (representing 37,2 ± 4,9% of total neurons per section; mean ± SD) is observed in the TG of *Prdm12*$^{LacZ/LacZ}$ pups, some of which being TrkB^{+}. By contrast, in control pups, only some rare tdTomato^{+} cells (neuronal and non-neuronal) and some tdTomato^{+} fibers could be observed, that have been suggested to be sympathetic in nature[30] (Figure S4C). To further assess the functional consequences of the ectopic activation of a VSN-like developmental program in TG of *Prdm12*$^{LacZ/LacZ}$ embryos, we next analyzed TG central and peripheral innervation pattern using a *Sox10*-Venus and/or *Phox2b*$^{Cre/+}$; *Rosa26*$^{LSL\text{-}tdTomato/+}$ reporter system.[4,20] At E13.5, the presence of tdTomato^{+} Peripherin^{+} fibers innervating the spinal trigeminal tract (sp5) revealed that *Prdm12*$^{LacZ/LacZ}$ tdTomato-labeled trigeminal neurons are able to properly reach their central target as would TG neurons (Peripherin^{+}) do in control embryos (Figure S4D). In the periphery, ectopic tdTomato signal could be observed in the maxillary and mandibular branches of the trigeminal nerve of *Prdm12*$^{LacZ/LacZ}$ embryos, respectively, innervating the nostril (among which the whisker pad) and jaw regions, the expected terminal locations for TG neurons

to innervate (Figure S4E). In order to determine if in TG of E18.5 *Prdm12*$^{LacZ/LacZ}$; *Phox2b*$^{Cre/+}$; *Rosa26*$^{LSL\text{-}tdTomato/+}$ embryos, late surviving tdTomato^{+} neurons effectively innervate the nostril region, we retrogradely labeled using NeuroVueJade dye[31,32] the upper lip and whisker pad innervating neurons. In TG of *Prdm12*$^{LacZ/LacZ}$, we found tdTomato^{+} neurons labeled with the NeuroVue dye indicating that neurons that express or have expressed Phox2b, however, project normally to their peripheral target (Figure S4F). Thus, the transient *Phox2b* expression is not sufficient to cause somatic neurons to shift to a complete visceral identity.

Prdm12 remains required in early post-mitotic nociceptive precursors to repress Phox2b and its ectopic expression in DRG does not cause a shift to an autonomic neuron identity

To determine whether in TG the persistent expression of *Prdm12* is required to repress Phox2a/b beyond the initial phase of neuronal specification, we conditionally inactivated *Prdm12* by crossing *Prdm12*$^{flox/flox}$ mice with *Advillin-Cre* mice that express the Cre recombinase from around E12.5 in developing sensory neurons.[33] Immunostaining analysis indicates that in *Advillin-Cre; Prdm12*$^{flox/flox}$ embryos, Prdm12 starts to be deleted in TG at E13.5 and that this deletion is effective by E14.5 (Figure S5A). In the hypoplastic TG of *Advillin-Cre; Prdm12*$^{flox/flox}$ embryos, we detected Phox2a^{+}, Phox2b^{+}, and Gata3^{+} neurons, as observed in *Prdm12*$^{LacZ/LacZ}$ embryos but in lower proportions (Figures S5B and S5C). These results show that Prdm12 is required from somatosensory neuron progenitors to early post-mitotic nociceptive precursors to repress *Phox2* genes.

In DRG of *Advillin-Cre; Prdm12*$^{flox/flox}$ embryos, Phox2a and Phox2b are ectopically expressed, as observed in TG (Figures S5D and S5E). As Phox2 genes are essential for the development of autonomic neurons in trunk NC cells, we asked whether their ectopic expression in *Advillin-Cre; Prdm12*$^{flox/flox}$ embryos switches on late markers of sympathetic neurons such as DBH and the norepinephrine transporter gene *Scl6a2*/NET.[34,35] Figures S5F and S5G show that none of these markers are detected in DRG of E14.5 *Advillin-Cre; Prdm12*$^{flox/flox}$ embryos. As expected from our RNAseq analysis, these markers are also undetectable in TG. Thus, DRG neurons ectopically expressing *Phox2* genes do not appear to acquire molecular characteristics of autonomic neurons. Together, these results reveal another mechanism by which Prdm12 promotes nociceptor fate in somatosensory progenitors, by repressing cells from engaging into an alternate Phox2a/b-driven gene program reminiscent in TG of the one at work in NG neurons.

Prdm12 functions as a context dependent repressor of visceral sensory neuron fate

As the data aforementioned demonstrate that Prdm12 is essential for the repression of Phox2b in developing sensory ganglia, we asked whether it is sufficient to block its endogenous expression in VSN. Therefore, we generated a transgenic mouse that can overexpress *Prdm12* in specific cell types at any desired age. A transgene containing the CAG promoter upstream of a *Lox-Stop-Lox-Prdm12-IRES-EGFP* (*LSL-Prdm12*) sequence was inserted into the *Rosa26* locus (Figure 6A). To validate this transgenic mouse line, we first crossed mice carrying the *Rosa26*$^{LSL\text{-}Prdm12}$ allele with *Dbx1*^{Cre} driver mice[36] which results in excision of the transcription stop sequence and permanent co-expression of Prdm12 and EGFP in p0 spinal ventral progenitors in which Prdm12 is normally not expressed. This Cre driver mouse line was chosen based on previous work that has shown that in the spinal cord Prdm12 is selectively expressed in p1 progenitors and promotes V1 interneuron development by repressing the expression of the transcription factor Dbx1, which is expressed in the adjacent p0 progenitor domain and promotes V0 interneuron fate.[37] We observed high levels of Cre-dependent recombination and Prdm12 expression, based on anti-EGFP and anti-Prdm12 immunofluorescence in the ventral spinal cord of *Dbx1*$^{Cre/+}$; *Rosa26*$^{LSL\text{-}Prdm12/+}$ embryos (Figure S6A). We next verified that the *Prdm12* transgene is functional by looking at the impact of Prdm12 ectopic expression on V0 and V1 interneurons development. We found that, as expected, the expression of *Dbx1* in p0 and that of the *Evx1* and Skor2 V0 markers[38] was reduced, while that of *En1* that labels V1 interneurons is expanded (Figures S6B and S6C). We then used this genetic tool to examine the effects of the ectopic expression of *Prdm12* on *Phox2b* in developing viscerosensory ganglia. Therefore, we crossed *Rosa26*$^{LSL\text{-}Prdm12}$ mice with *Phox2b*^{Cre} mice,[4] and performed immunostaining on head sections of E11.5-E13.5 embryos. In E11.5 *Phox2b*$^{Cre/+}$; *Rosa26*$^{LSL\text{-}Prdm12/+}$ embryos, we observed ectopic expression of Prdm12 in the GG and the PNG. However, Phox2b expression appeared unaffected in these different VSN ganglia (Figures 6B and 6C). To test the hypothesis that Prdm12 may be unable to downregulate *Phox2b* because *Prdm12* is turned on later than *Phox2b* in Phox2b^{+} precursors, after the choice of precursors to adopt a visceral sensory neuron fate has been taken, we also crossed *Rosa26*$^{LSL\text{-}Prdm12}$ mice with *Wnt1*-Cre mice that drive Cre expression into NC cells. In E13.5 *Wnt1*-Cre; *Rosa26*$^{LSL\text{-}Prdm12/+}$ embryos, we observed an ectopic expression of Prdm12 in sympathetic ganglia (SG). We found that in SG, Phox2b was also not affected by Prdm12 overexpression (Figure 6D). Thus, although required to repress *Phox2b* in somatosensory ganglia, *Prdm12* ectopic expression is not sufficient to repress it in VSN or SG, indicating its activity is highly dependent of the cellular context.

Prdm12 is not required in late differentiating and mature nociceptors to repress *Phox2* genes but continues to play a role in the maintenance of some aspects of their molecular identity

In a previous work, we analyzed by RNA-seq the transcriptome of TG and DRG of *Rosa26*^{CreERT2}; *Prdm12*$^{flox/flox}$ adult mice treated with tamoxifen.[39] In the list of common upregulated DEGs, although neither Phox2a nor Phox2b could be detected, we found a few genes upregulated by the loss of *Prdm12*[39] (Figure 7A). Among them are *Agtr1a* encoding a receptor for the neuropeptide angiotensin[40] expressed in DRG in non-peptidergic nociceptors, the neurotrophic receptor *Ntrk3*/TrkC[23] enriched in LTMRs, *Skor2* encoding a ski family member transcriptional cofactor (also designated Corl2)[41] expressed in LTMRs and *Stk32a* encoding the serine/threonine kinase 32A that is only weakly expressed in DRG, mainly in non-peptidergic nociceptors.[23] While *Agtr1a* and *Ntrk3*/TrkC are both also expressed in some NG neurons,[26] all four genes are detected in sympathetic neurons.[24,42] We examined the expression of these markers in *Nav1.8*^{Cre}; *Prdm12*$^{flox/flox}$ mice that allow deletion

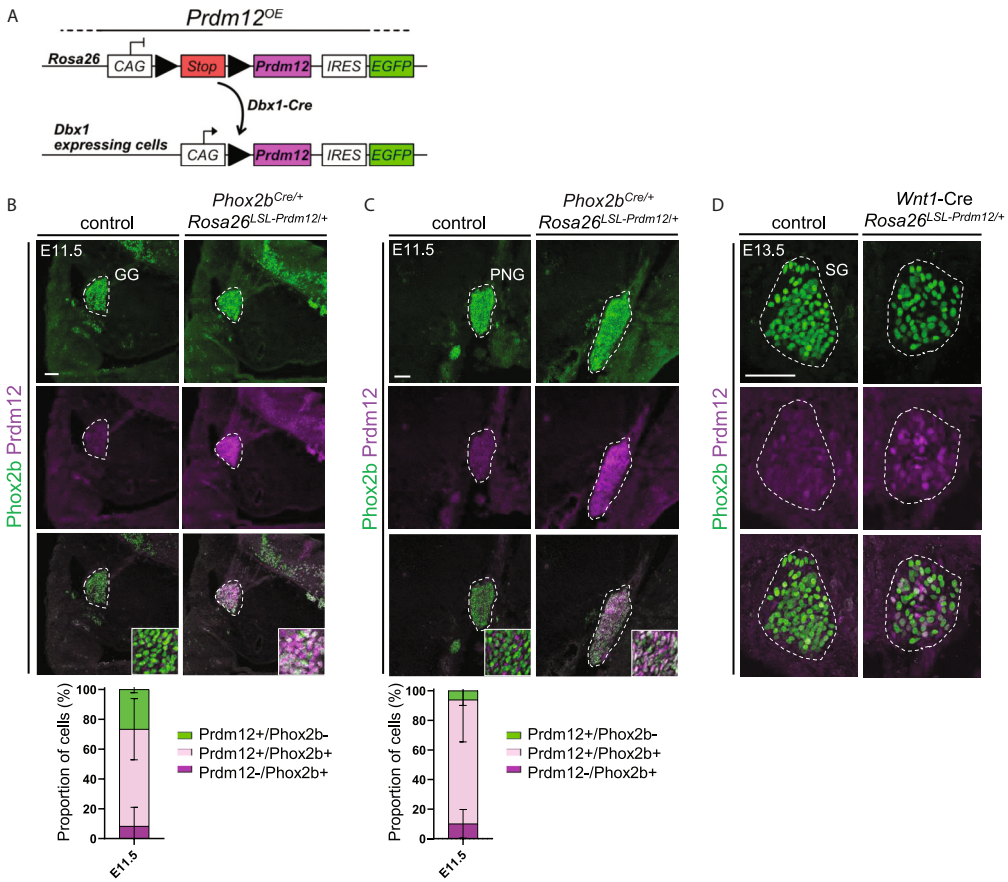

Figure 6. Prdm12 ectopic expression is not sufficient to repress Phox2b expression in visceral ganglia of the PNS

(A) Schematic of the inducible *Rosa26*$^{LSL\text{-}Prdm12}$ locus allowing expression of Prdm12 and EGFP in a Cre-inducible manner.

(B and C) Immunostainings with Phox2b and Prdm12 antibodies on coronal sections through GG (A) and PNG (B) of E11.5 *Phox2b*$^{Cre/+}$; *Rosa26*$^{LSL\text{-}Prdm12/+}$ and control embryos. Insets show magnifications of the indicated area. Histograms show quantifications of the immunostainings.

(D) Immunostainings of Phox2b and Prdm12 on coronal sections through SG from E13.5 *Wnt1*-Cre; *Rosa26*$^{LSL\text{-}Prdm12/+}$ and control embryos. PNG, petrosal-nodose ganglia; GG, geniculate ganglia; SG, sympathetic ganglia. Scale bars, 50 μm.

of *Prdm12* in nociceptors at perinatal stage[43] and in *Rosa26*^{CreERT2}; *Prdm12*$^{flox/flox}$ mice expressing a ubiquitous tamoxifen dependent Cre recombinase. Figures 7B, 7C shows that the number of Skor2^{+} and TrkC^{+} neurons is increased in DRG of both *Nav1.8*$^{Cre/+}$; *Prdm12*$^{flox/flox}$ and *Rosa26*$^{CreERT2/+}$; *Prdm12*$^{flox/flox}$ mice. Upregulation of *Stk32a* and *Agtr1a* was also visible in DRG of *Rosa26*$^{CreERT2/+}$; *Prdm12*$^{flox/flox}$ mice (Figure 7C). Although none of these markers are specific of sympathetic neurons, these results suggest that Prdm12, independently of its repressive action on Phox2b, prevents mature nociceptors to express markers of autonomous neurons.

DISCUSSION

Congenital insensitivity to pain (CIP) is rare autosomal recessive genetic disorders in which a person cannot feel pain from birth, due to either undeveloped nociceptors or non-functional nociceptors. *PRDM12* that encodes a transcriptional regulator, is one of the very few genes whose mutations cause CIP,[44] due to is requirement for the initiation of the nociceptive lineage.[11–13] Besides CIP, biallelic polyalanine expansions in PRDM12 have been described resulting in a milder, more localized congenital sensory disorder, designated Midface Toddler Excoriation Syndrome (MiTES). MiTES is a condition reported in children characterized by severe midfacial lesions resulting from itch-induced excessive scratching with little if any evidence of generalized pain insensitivity.[45] How expansions of the PRDM12 polyalanine tract lead to cranial specific nociceptor dysfunction is not known. Therefore, in this study, we have pursued our efforts to better understand the consequences of the loss of Prdm12 on sensory neuron differentiation, with a focus on cranial ganglia.

Here, we show that in the absence of Prdm12, TG, and DRG hypoplasia observed in *Prdm12* knockout embryos is partially rescued in a *Bax*$^{-/-}$ background, confirming the importance of Prdm12 for cell survival. Other studies have proposed that the absence of nociceptors was mainly due to defective proliferation rather than increased cell death.[12,13] The origin of this discrepancy is unclear. Differences in strain used or stages/number of animals examined, retention of *Prdm12* exon II to V in the conditional knockout in the study by Landy et al., 2021,

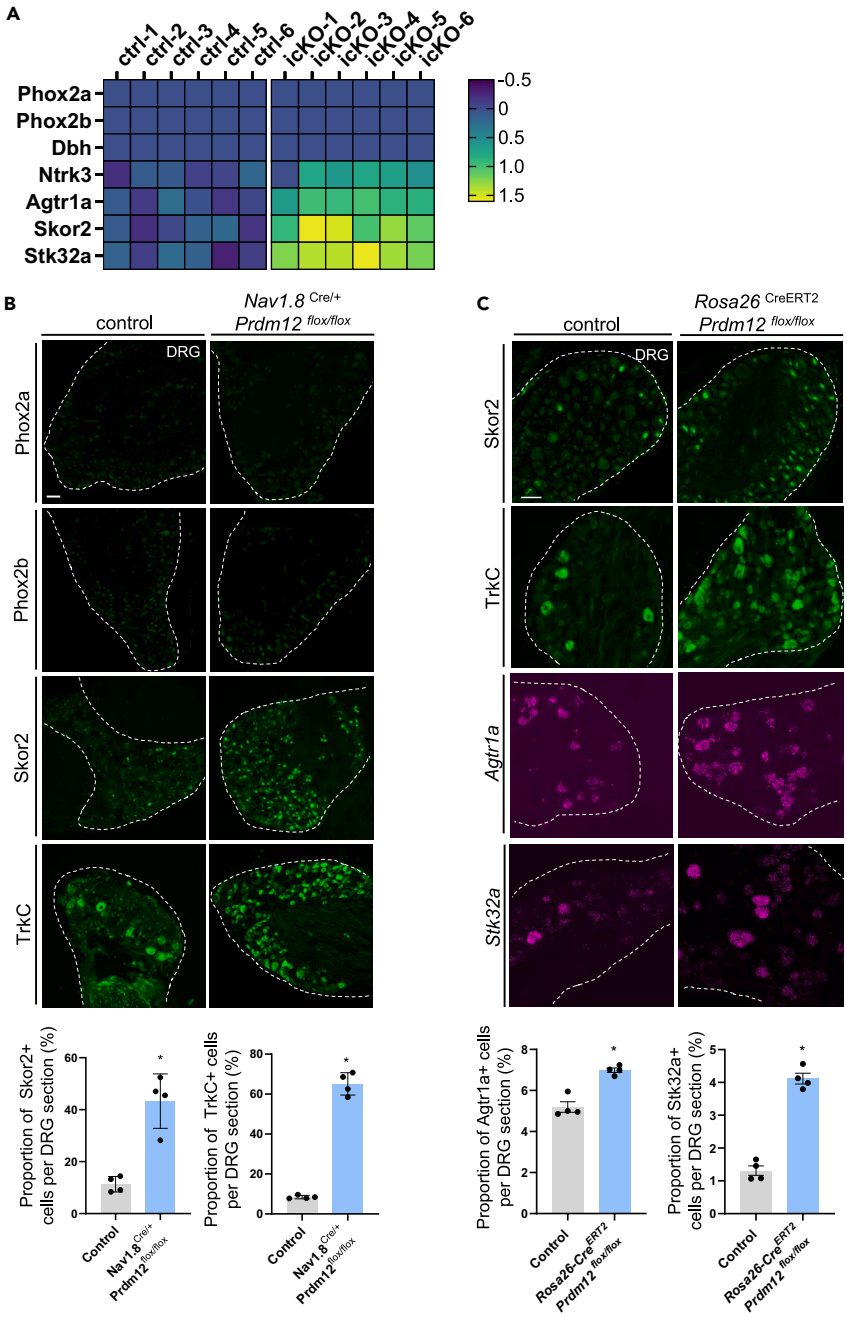

Figure 7. In perinatal and adult somatosensory neurons, Prdm12 continues to play a role in the maintenance of their molecular identity

(A) Heatmap depicting RNA-seq Log2 Fold Change expression level of selected genes in thoracic DRG collected from adult *Rosa26*^{CreERT2}; *Prdm12*$^{flox/flox}$ (icKO) and control (ctrl) mice one month after tamoxifen injection normalized to the mean Log2 Fold Change of control replicates (Latragna et al., 2022).

(B) Immunostainings on cross-sections through DRG of E18.5 *Nav1.8*$^{Cre/+}$; *Prdm12*$^{flox/flox}$ embryos revealing absence of ectopic Phox2a/b^{+} cells and increased number of Skor2^{+} and TrkC^{+} cells in the absence of *Prdm12* expression. Graphs showing quantification of the numbers of positive cells detected are shown.

(C) Immunostainings and RNAscope based *in situ* hybridization revealing increased number of Skor2^{+}, TrkC^{+}, *Agtr1a*$^{+}$ and *Stk32a*$^{+}$ cells on cross-sections through DRG of *Rosa26*^{CreERT2}; *Prdm12*$^{flox/flox}$ and *Rosa26*$^{CreERT2/CreERT2}$ adult mice. Histograms are represented as mean ± standard error of mean (SEM). Each dot in histograms represents the mean values obtained for an individual biological replicate. Mann-Whitney tests have been applied. Calculated p values are referred to as follow: *p < 0,05; **p < 0,01; ***p < 0.001 and ns for non-significant difference (p > 0,05). Scale bars, 50 μm. DRG, dorsal root ganglia.

may be variables explaining those discrepancies. SJG development was in contrast not rescued at all by Bax deletion suggesting that Prdm12 may control its formation via other mechanisms. Whether these ganglia fail to develop because of defects in NC migration, proliferation, and/or specification remains to be further studied.

Phox2 factors act as master regulators of the entire visceral reflex neuronal circuits that control the digestive, cardiovascular, and respiratory systems. Indeed, within the PNS, on the efferent paths, *Phox2* genes are essential for the development of the autonomic ganglia (sympathetic, parasympathetic, and enteric). On the afferent paths, Phox2 transcription factors control the differentiation of the neurons of the three epibranchial placode derived ganglia (geniculate, petrosal, and nodose). In their absence, visceral neurons change fate and acquire a somatic molecular identity.[4] We report that upon the loss of Prdm12 some SSN before undergoing apoptosis start to express the homeobox transcription factor Phox2b and its paralog Phox2a, which likely extend their survival. To date, no such phenotype has been observed in sensory ganglia of embryos knock-out for the other regulators of somatosensory neurogenesis. To our knowledge, only the homeobox transcription factor Lbx1 has a similar function reported in relay neurons in the hindbrain.[46] When examining *Prdm12* expression in the PNG of *Phox2b*$^{LacZ/LacZ}$ embryos, we found that it is not ectopically expressed as initially reported for *Pou4f1*,[4] suggesting that the visceral-to-somatic transition observed in *Phox2b*$^{LacZ/LacZ}$ may not be complete (Figure S7), which remains to be further investigated.

In developing TG, we show that some of those ectopic Phox2b^{+} neurons are eliminated with time and that changes in response to the ectopic activation of Phox2b in TG are limited. Indeed, (i) only a limited number of markers specifically enriched in VSN were found upregulated in our transcriptomic analyses of TG of *Prdm12* knockout embryos; (ii) ectopic Phox2b^{+} neurons that survive around birth in TG of *Prdm12* knockout embryos show central and peripheral projections typical of SSN and (iii) the somatic determinant Brn3a was still expressed in ectopic Phox2b^{+} neurons. Brn3a plays essential functions in developing sensory neurons as, like Prdm12, the repression of gene programs characteristic of other tissues (including non-neuronal ones such as cardiac/cranial mesoderm).[47] Its unaltered expression in SSN of *Prdm12* knockout embryos may likely explain some of their preserved SSN features. These data further suggest that in cranial sensory pathways, visceral and somatic sensory fates are related.[4] Whether alterations of the fate of SSN in developing TG ganglia as reported in this study also occur in MiTES patients and are responsible for their facial altered sensitivity remains to be investigated. Besides this cell autonomous function of Prdm12 in TG progenitors in the choice between somatic or visceral sensory fate, we also observed defects in *Prdm12*$^{lacZ/lacZ}$ embryos in the localization of a pool of hindbrain Phox2b^{+} Nkx6.1^{+} branchio-visceral motoneurons.[8,28,29] How the loss of nociceptive fibers indirectly affects the migration of these branchio-motor neurons and whether it has any consequence on the formation of other PNS structures remains unknown.

In DRG, our results indicate that the constitutive or conditional loss of *Prdm12* also leads to an upregulation of *Phox2* genes. In *Advillin-Cre; Prdm12*$^{flox/flox}$ embryos, despite the ectopic expression of *Phox2b*, cells do, however, not acquire an autonomic fate. Forced *Phox2* gene expression using retroviral vectors in trunk NC cultures and in DRG of chick embryos has been shown, however, to be sufficient to promote sympathetic neuron generation.[48] As *Phox2* genes are expressed throughout embryonic sympathetic neuron development and as continued expression of *Phox2b* during differentiation has been shown to be required in SG,[34,49] it is likely the transient nature and late onset of the ectopic *Phox2b* expression observed in DRG of *Prdm12*$^{lacZ/lacZ}$ embryos that explains the inability of NC cells to acquire characteristics of sympathetic neurons. It has been shown recently that trunk NC cells differentiate in a stepwise manner through a series of binary lineage restriction decisions. A first phase of decision occurs in progenitors that separates sensory neuro-glial (and melanocyte fates) from bipotent autonomic-mesenchymal fated cells. A second later decision occurs in trunk NC cells that separate cells adopting an autonomic fate from others acquiring a mesenchymal fate.[50] Applying our data to this model would suggest that Prdm12 is involved in both of these lineage bifurcations, acting first with proneural factors[11] to promote a sensory (nociceptive) fate and later through its ability to repress *Phox2b* to block autonomic neuron differentiation.

By temporally controlling Prdm12 inactivation, we found that its ongoing expression in DRG is still required to repress *Phox2b* in early differentiating postmitotic nociceptive neurons and that this is no longer the case in late differentiating and mature nociceptors of adult mice. Interestingly, in mature nociceptors of adult mice, we showed that loss of *Prdm12* still upregulates a few markers related to autonomous neurons. As these markers are not selective of autonomous neurons only, further studies are, however, needed to define the precise molecular changes that occurs upon loss of *Prdm12* in mature nociceptors. This is an important question given the potential of Prdm12 as a target for the development of novel analgesics.[51]

Transcription factors are essential determinants of cell fate acquisition and stability. They mediate their role via direct DNA binding to regulate transcription and chromatin accessibility. Transcription factors can act as lineage switches by activating cell-type specific transcriptional programs or by repressing the programs of alternative lineages.[52,53] How Prdm12 controls the expression of its targets, promoting *Ntrk1*/TrkA and repressing *Phox2b* expression in developing nociceptors remains unknown. Our data and that of others suggest that at least in some context Prdm12 acts as an epigenetic repressor or corepressor, via the recruitment of the histone methyltransferase EHMT2/G9a or other corepressors.[37,54,55] Whether Prdm12 directly represses *Phox2b* transcription as part of a transcriptional repressive complex binding to the *Phox2b* locus or alternatively, whether the ectopic expression of *Phox2b* may be secondary to another transcriptional abnormality resulting from the absence of *Prdm12* remains to be addressed. Our observation that Prdm12 is not sufficient to repress *Phox2* genes in VSN supports the idea that Prdm12 needs an appropriate permissive environment or dedicated partners to repress its targets. Defining its interactome in sensory neurons will thus be of paramount importance to understand its mechanism of action in somatosensory neurogenesis.

Limitations of the study

While this study provides further evidence for the importance of Prdm12 in the survival of developing nociceptors and demonstrates that it is also required to prevent precursors to engage into an alternate Phox2 driven visceral neuronal type differentiation program, its mechanism of

action remains unknown. It remains unclear whether Prdm12 directly represses Phox2 and directly activates TrkA, whether it has sequence-specific DNA binding capacity, and how it acts as an epigenetic regulator to control chromatin landscape. These are important questions for future studies. In nociceptors in which Prdm12 is inactivated conditionally at the adult stage, we identified several markers expressed in autonomic neurons that are upregulated independently of Phox2b suggesting that Prdm12 plays a role in the stability of the nociceptive fate. However, because none of them are selective to autonomic neurons, further studies are needed to define the molecular function of *Prdm12* in mature nociceptors.

STAR★METHODS

Detailed methods are provided in the online version of this paper and include the following:

- KEY RESOURCES TABLE
- RESOURCE AVAILABILITY
  - Lead contact
  - Materials availability
  - Data and code availability
- EXPERIMENTAL MODEL AND STUDY PARTICIPANT DETAILS
  - Mice
- METHOD DETAILS
  - Embryo processing
  - Tamoxifen treatment
  - *In situ* hybridizations and immunostainings
  - NeuroVueJade retro labeling
  - RNAscope
  - X-gal staining on embryo sections
  - RNA sequencing and data processing
- QUANTIFICATION AND STATISTICAL ANALYSIS

SUPPLEMENTAL INFORMATION

Supplemental information can be found online at https://doi.org/10.1016/j.isci.2023.108364.

ACKNOWLEDGMENTS

We are grateful to E. Bourinet, A. Pattyn, L. Nguyen, A. Pierani, for providing mouse lines, A. Pattyn for providing the DBH probe and T. Müller and L. Reichardt for the Tlx3 and TrkA antibodies. We thank M. Luypaert, L. Gentile, and L. Delhaye for their technical help at the mouse facility. We also thank former master students E. Malki and E. Acedo Reina for their help to repeat some of the experiments. We are grateful to members of the Center for Microscopy and Molecular Imaging (CMMI) for their help with microscopy. This work was supported by grants from the Walloon Region (Win2wal project PANOPP 1810123 and the FNRS (PDR T.0020.20 and T.0012.22). S.V. and S.D. are FRS-FNRS post-doctoral fellows. P.C. is a WBI (Wallonie-Bruxelles International) postdoctoral researcher. M.D. and A.S. are fellows from the FNRS (supported by FRIA and Aspirant fellowships, respectively).

AUTHOR CONTRIBUTIONS

S.V., M.D., P.C., S.D., A.S., and Y.A. performed the molecular and biological experiments, with the help of S.K. for cloning and ISH. M.S. and G.S.-R. performed the RNA-sequencing and raw analysis of the data. S.V., P.C., S.D., and E.J.B. wrote the manuscript. All authors analyzed the data and/or commented the manuscript. E.J.B. conceived and supervised the study.

DECLARATION OF INTERESTS

The authors declare no competing interests.

INCLUSION AND DIVERSITY

We support inclusive, diverse, and equitable conduct of research.

Received: September 29, 2023
Revised: October 13, 2023
Accepted: October 26, 2023
Published: October 31, 2023

REFERENCES

1. Kandel, E., Koester, J., Mack, S., and Siegelbaum, S. (2021). Principles of Neural Science, 6th ed. (McGraw-Hill).
2. Nomaksteinsky, M., Kassabov, S., Chettouh, Z., Stoeklé, H.C., Bonnaud, L., Fortin, G., Kandel, E.R., and Brunet, J.-F. (2013). Ancient origin of somatic and visceral neurons. BMC Biol. *11*, 53. https://doi.org/10.1186/1741-7007-11-53.
3. Bertucci, P., and Arendt, D. (2013). Somatic and visceral nervous systems - an ancient duality. BMC Biol. *11*, 54. https://doi.org/10.1186/1741-7007-11-54.
4. D'Autréaux, F., Coppola, E., Hirsch, M.R., Birchmeier, C., and Brunet, J.F. (2011). Homeoprotein Phox2b commands a somatic-to-visceral switch in cranial sensory pathways. Proc. Natl. Acad. Sci. USA *108*, 20018–20023. https://doi.org/10.1073/pnas.1110416108.
5. Vermeiren, S., Bellefroid, E.J., and Desiderio, S. (2020). Vertebrate Sensory Ganglia: Common and Divergent Features of the Transcriptional Programs Generating Their Functional Specialization. Front. Cell Dev. Biol. *8*, 587699. https://doi.org/10.3389/fcell.2020.587699.
6. Morin, X., Cremer, H., Hirsch, M.R., Kapur, R.P., Goridis, C., and Brunet, J.F. (1997). Defects in sensory and autonomic ganglia and absence of locus coeruleus in mice deficient for the homeobox gene Phox2a. Neuron *18*, 411–423. https://doi.org/10.1016/S0896-6273(00)81242-8.
7. Pattyn, A., Morin, X., Cremer, H., Goridis, C., and Brunet, J.F. (1999). The homeobox gene Phox2b is essential for the development of autonomic neural crest derivatives. Nature *399*, 366–370. https://doi.org/10.1038/20700.
8. Pattyn, A., Hirsch, M., Goridis, C., and Brunet, J.-F. (2000). Control of hindbrain motor neuron differentiation by the homeobox gene Phox2b. Development *127*, 1349–1358. https://doi.org/10.1242/dev.127.7.1349.
9. Coppola, E., Pattyn, A., Guthrie, S.C., Goridis, C., and Studer, M. (2005). Reciprocal gene replacements reveal unique functions for Phox2 genes during neural differentiation. EMBO J. *24*, 4392–4403. https://doi.org/10.1038/sj.emboj.7600897.
10. Ruffault, P.-L., D'Autréaux, F., Hayes, J.A., Nomaksteinsky, M., Autran, S., Fujiyama, T., Hoshino, M., Hägglund, M., Kiehn, O., Brunet, J.-F., et al. (2015). The retrotrapezoid nucleus neurons expressing Atoh1 and Phox2b are essential for the respiratory response to CO2. Elife *4*, e07051. https://doi.org/10.7554/eLife.07051.
11. Desiderio, S., Vermeiren, S., Van Campenhout, C., Kricha, S., Malki, E., Richts, S., Fletcher, E.V., Vanwelden, T., Schmidt, B.Z., Henningfeld, K.A., et al. (2019). Prdm12 Directs Nociceptive Sensory Neuron Development by Regulating the Expression of the NGF Receptor TrkA. Cell Rep. *26*, 3522–3536.e5. https://doi.org/10.1016/j.celrep.2019.02.097.
12. Bartesaghi, L., Wang, Y., Fontanet, P., Wanderoy, S., Berger, F., Wu, H., Akkuratova, N., Bouçanova, F., Médard, J.J., Petitpré, C., et al. (2019). PRDM12 Is Required for Initiation of the Nociceptive Neuron Lineage during Neurogenesis. Cell Rep. *26*, 3484–3492.e4. https://doi.org/10.1016/j.celrep.2019.02.098.
13. Landy, M.A., Goyal, M., Casey, K.M., Liu, C., and Lai, H.C. (2021). Loss of Prdm12 during development, but not in mature nociceptors, causes defects in pain sensation. Cell Rep. *34*, 108913. https://doi.org/10.1016/j.celrep.2021.108913.
14. Chen, Y.C., Auer-Grumbach, M., Matsukawa, S., Zitzelsberger, M., Themistocleous, A.C., Strom, T.M., Samara, C., Moore, A.W., Cho, L.T.Y., Young, G.T., et al. (2015). Transcriptional regulator PRDM12 is essential for human pain perception. Nat. Genet. *47*, 803–808. https://doi.org/10.1038/ng.3308.
15. Kim, J., Lo, L., Dormand, E., and Anderson, D.J. (2003). SOX10 maintains multipotency and inhibits neuronal differentiation of neural crest stem cells. Neuron *38*, 17–31. https://doi.org/10.1016/S0896-6273(03)00163-6.
16. Sun, Y., Dykes, I.M., Liang, X., Eng, S.R., Evans, S.M., and Turner, E.E. (2008). A central role for Islet1 in sensory neuron development linking sensory and spinal gene regulatory programs. Nat. Neurosci. *11*, 1283–1293. https://doi.org/10.1038/nn.2209.
17. Ma, Q., Fode, C., Guillemot, F., and Anderson, D.J. (1999). NEUROGENIN1 and NEUROGENIN2 control two distinct waves of neurogenesis in developing dorsal root ganglia. Genes Dev. *13*, 1717–1728. https://doi.org/10.1101/gad.13.13.1717.
18. Ma, Q., Chen, Z., del Barco Barrantes, I., De La Pompa, J.L., and Anderson, D.J. (1998). neurogenin1 is essential for the determination of neuronal precursors for proximal cranial sensory ganglia. Neuron *20*, 469–482. https://doi.org/10.1016/S0896-6273(00)80988-5.
19. Takano-Maruyama, M., Chen, Y., and Gaufo, G.O. (2012). Differential contribution of Neurog1 and Neurog2 on the formation of cranial ganglia along the anterior-posterior axis. Dev. Dyn. *241*, 229–241. https://doi.org/10.1002/dvdy.22785.
20. Shibata, S., Yasuda, A., Renault-Mihara, F., Suyama, S., Katoh, H., Inoue, T., Inoue, Y.U., Nagoshi, N., Sato, M., Nakamura, M., et al. (2010). Sox10-Venus mice: a new tool for real-time labeling of neural crest lineage cells and oligodendrocytes. Mol. Brain *3*, 31. https://doi.org/10.1186/1756-6606-3-31.
21. White, F.A., Keller-Peck, C.R., Knudson, C.M., Korsmeyer, S.J., and Snider, W.D. (1998). Widespread Elimination of Naturally Occurring Neuronal Death in Bax-Deficient Mice. J. Neurosci. *18*, 1428–1439. https://doi.org/10.1523/JNEUROSCI.18-04-01428.1998.
22. Patel, T.D., Jackman, A., Rice, F.L., Kucera, J., and Snider, W.D. (2000). Development of sensory neurons in the absence of NGF/TrkA signaling in vivo. Neuron *25*, 345–357. https://doi.org/10.1016/S0896-6273(00)80899-5.
23. Usoskin, D., Furlan, A., Islam, S., Abdo, H., Lönnerberg, P., Lou, D., Hjerling-Leffler, J., Haeggström, J., Kharchenko, O., Kharchenko, P.V., et al. (2015). Unbiased classification of sensory neuron types by large-scale single-cell RNA sequencing. Nat. Neurosci. *18*, 145–153. https://doi.org/10.1038/nn.3881.
24. Zeisel, A., Hochgerner, H., Lönnerberg, P., Johnsson, A., Memic, F., van der Zwan, J., Häring, M., Braun, E., Borm, L.E., La Manno, G., et al. (2018). Molecular Architecture of the Mouse Nervous System. Cell *174*, 999–1014.e22. https://doi.org/10.1016/j.cell.2018.06.021.
25. Kaelberer, M.M., Caceres, A.I., and Jordt, S.-E. (2020). Activation of a nerve injury transcriptional signature in airway-innervating sensory neurons after lipopolysaccharide-induced lung inflammation. Am. J. Physiol. Lung Cell Mol. Physiol. *318*, L953–L964. https://doi.org/10.1152/ajplung.00403.2019.
26. Kupari, J., Häring, M., Agirre, E., Castelo-Branco, G., and Ernfors, P. (2019). An Atlas of Vagal Sensory Neurons and Their Molecular Specialization. Cell Rep. *27*, 2508–2523.e4. https://doi.org/10.1016/j.celrep.2019.04.096.
27. Pattyn, A., Morin, X., Cremer, H., Goridis, C., and Brunet, J.F. (1997). Expression and interactions of the two closely related homeobox genes Phox2a and Phox2b during neurogenesis. Development *124*, 4065–4075.
28. Pattyn, A., Vallstedt, A., Dias, J.M., Sander, M., and Ericson, J. (2003). Complementary roles for Nkx6 and Nkx2 class proteins in the establishment of motoneuron identity in the hindbrain. Development *130*, 4149–4159. https://doi.org/10.1242/dev.00641.
29. Müller, M., Jabs, N., Lorke, D.E., Fritzsch, B., and Sander, M. (2003). Nkx6.1 controls migration and axon pathfinding of cranial branchio-motoneurons. Development *130*, 5815–5826. https://doi.org/10.1242/dev.00815.
30. Ohman-Gault, L., Huang, T., and Krimm, R. (2017). The transcription factor Phox2b distinguishes between oral and non-oral sensory neurons in the geniculate ganglion. J. Comp. Neurol. *525*, 3935–3950. https://doi.org/10.1002/cne.24312.
31. Jensen-Smith, H., Gray, B., Muirhead, K., Ohlsson-Wilhelm, B., and Fritzsch, B. (2007). Long-Distance Three-Color Neuronal Tracing in Fixed Tissue Using NeuroVue Dyes. Immunol. Invest. *36*, 763–789. https://doi.org/10.1080/08820130701706711.
32. Matsubayashi, Y., Iwai, L., and Kawasaki, H. (2008). Fluorescent double-labeling with carbocyanine neuronal tracing and immunohistochemistry using a cholesterol-specific detergent digitonin. J. Neurosci. Methods *174*, 71–81. https://doi.org/10.1016/j.jneumeth.2008.07.003.
33. Zhou, X., Wang, L., Hasegawa, H., Amin, P., Han, B.-X., Kaneko, S., He, Y., and Wang, F. (2010). Deletion of PIK3C3/Vps34 in sensory neurons causes rapid neurodegeneration by disrupting the endosomal but not the autophagic pathway. Proc. Natl. Acad. Sci. USA *107*, 9424–9429. https://doi.org/10.1016/j.applthermaleng.2011.10.001.
34. Ernsberger, U., and Rohrer, H. (2018). Sympathetic tales: Subdivisons of the autonomic nervous system and the impact of developmental studies. Neural Dev. *13*, 20. https://doi.org/10.1186/s13064-018-0117-6.
35. Wu, H.-F., Yu, W., Saito-Diaz, K., Huang, C.-W., Carey, J., Lefcort, F., Hart, G.W., Liu, H.-X., and Zeltner, N. (2022). Norepinephrine transporter defects lead to sympathetic hyperactivity in Familial Dysautonomia models. Nat. Commun. *13*, 7032. https://doi.org/10.1038/s41467-022-34811-7.
36. Bielle, F., Griveau, A., Narboux-Nême, N., Vigneau, S., Sigrist, M., Arber, S., Wassef, M., and Pierani, A. (2005). Multiple origins of Cajal-Retzius cells at the borders of the developing pallium. Nat. Neurosci. *8*, 1002–1012. https://doi.org/10.1038/nn1511.
37. Thélie, A., Desiderio, S., Hanotel, J., Quigley, I., Van Driessche, B., Rodari, A., Borromeo, M.D., Kricha, S., Lahaye, F., Croce, J., et al. (2015). Prdm12 specifies V1 interneurons through cross-repressive interactions with Dbx1 and Nkx6 genes in Xenopus.

Development (Camb.) *142*, 3416–3428. https://doi.org/10.1242/dev.121871.
38. Juárez-Morales, J.L., Schulte, C.J., Pezoa, S.A., Vallejo, G.K., Hilinski, W.C., England, S.J., de Jager, S., and Lewis, K.E. (2016). Evx1 and Evx2 specify excitatory neurotransmitter fates and suppress inhibitory fates through a Pax2-independent mechanism. Neural Dev. *11*, 5. https://doi.org/10.1186/s13064-016-0059-9.
39. Latragna, A., Sabaté San José, A., Tsimpos, P., Vermeiren, S., Gualdani, R., Chakrabarti, S., Callejo, G., Desiderio, S., Shomroni, O., Sitte, M., et al. (2022). Prdm12 modulates pain-related behavior by remodeling gene expression in mature nociceptors. Pain *163*, e927–e941. https://doi.org/10.1097/j.pain.0000000000002536.
40. Gallo-Payet, N., Guimond, M.-O., Bilodeau, L., Wallinder, C., Alterman, M., and Hallberg, A. (2011). Angiotensin II, a Neuropeptide at the Frontier between Endocrinology and Neuroscience: Is There a Link between the Angiotensin II Type 2 Receptor and Alzheimer's Disease? Front. Endocrinol. *2*, 17. https://doi.org/10.3389/fendo.2011.00017.
41. Nakatani, T., Minaki, Y., Kumai, M., Nitta, C., and Ono, Y. (2014). The c-Ski family member and transcriptional regulator Corl2/Skor2 promotes early differentiation of cerebellar Purkinje cells. Dev. Biol. *388*, 68–80. https://doi.org/10.1016/j.ydbio.2014.01.016.
42. Liu, S., Xiang, K., Yuan, F., and Xiang, M. (2023). Generation of self-organized autonomic ganglion organoids from fibroblasts. iScience *26*, 106241. https://doi.org/10.1016/j.isci.2023.106241.
43. Stirling, L.C., Forlani, G., Baker, M.D., Wood, J.N., Matthews, E.A., Dickenson, A.H., and Nassar, M.A. (2005). Nociceptor-specific gene deletion using heterozygous NaV1.8-Cre recombinase mice. Pain *113*, 27–36. https://doi.org/10.1016/j.pain.2004.08.015.
44. Nahorski, M.S., Chen, Y.C., and Woods, C.G. (2015). New Mendelian Disorders of Painlessness. Trends Neurosci. *38*, 712–724. https://doi.org/10.1016/j.tins.2015.08.010.
45. Moss, C., Srinivas, S.M., Sarveswaran, N., Nahorski, M., Gowda, V.K., Browne, F.M., and Woods, G. (2018). Midface toddler excoriation syndrome (MiTES) can be caused by autosomal recessive biallelic mutations in a gene for congenital insensitivity to pain, PRDM12. Br. J. Dermatol. *179*, 1135–1140. https://doi.org/10.1111/bjd.16893.
46. Sieber, M.A., Storm, R., Martinez-de-la-Torre, M., Müller, T., Wende, H., Reuter, K., Vasyutina, E., and Birchmeier, C. (2007). Lbx1 Acts as a Selector Gene in the Fate Determination of Somatosensory and Viscerosensory Relay Neurons in the Hindbrain. J. Neurosci. *27*, 4902–4909. https://doi.org/10.1523/JNEUROSCI.0717-07.2007.
47. Lanier, J., Dykes, I.M., Nissen, S., Eng, S.R., and Turner, E.E. (2009). Brn3a regulates the transition from neurogenesis to terminal differentiation and represses non-neural gene expression in the trigeminal ganglion. Dev. Dyn. *238*, 3065–3079. https://doi.org/10.1002/dvdy.22145.
48. Stanke, M., Junghans, D., Geissen, M., Goridis, C., Ernsberger, U., and Rohrer, H. (1999). The Phox2 homeodomain proteins are sufficient to promote the development of sympathetic neurons. Development *126*, 4087–4094. https://doi.org/10.1242/dev.126.18.4087.
49. Coppola, E., d'Autréaux, F., Rijli, F.M., and Brunet, J.F. (2010). Ongoing roles of Phox2 homeodomain transcription factors during neuronal differentiation. Development *137*, 4211–4220. https://doi.org/10.1242/dev.056747.
50. Soldatov, R., Kaucka, M., Kastriti, M.E., Petersen, J., Chontorotzea, T., Englmaier, L., Akkuratova, N., Yang, Y., Häring, M., Dyachuk, V., et al. (2019). Spatiotemporal structure of cell fate decisions in murine neural crest. Science *364*, eaas9536. https://doi.org/10.1126/science.aas9536.
51. Imhof, S., Kokotović, T., and Nagy, V. (2020). PRDM12: New Opportunity in Pain Research. Trends Mol. Med. *26*, 895–897. https://doi.org/10.1016/j.molmed.2020.07.007.
52. Stadhouders, R., Filion, G.J., and Graf, T. (2019). Transcription factors and 3D genome conformation in cell-fate decisions. Nature *569*, 345–354. https://doi.org/10.1038/s41586-019-1182-7.
53. Kutejova, E., Sasai, N., Shah, A., Gouti, M., and Briscoe, J. (2016). Neural Progenitors Adopt Specific Identities by Directly Repressing All Alternative Progenitor Transcriptional Programs. Dev. Cell *36*, 639–653. https://doi.org/10.1016/j.devcel.2016.02.013.
54. Yang, C.M., and Shinkai, Y. (2013). Prdm12 is induced by retinoic acid and exhibits anti-proliferative properties through the cell cycle modulation of P19 embryonic carcinoma cells. Cell Struct. Funct. *38*, 197–206. https://doi.org/10.1247/csf.13010.
55. Yildiz, O., Downes, G.B., and Sagerström, C.G. (2019). Zebrafish prdm12b acts independently of nkx6.1 repression to promote eng1b expression in the neural tube p1 domain. Neural Dev. *14*, 5. https://doi.org/10.1186/s13064-019-0129-x.
56. Madisen, L., Zwingman, T.A., Sunkin, S.M., Oh, S.W., Zariwala, H.A., Gu, H., Ng, L.L., Palmiter, R.D., Hawrylycz, M.J., Jones, A.R., et al. (2010). A robust and high-throughput Cre reporting and characterization system for the whole mouse brain. Nat. Neurosci. *13*, 133–140. https://doi.org/10.1038/nn.2467.
57. Ventura, A., Kirsch, D.G., McLaughlin, M.E., Tuveson, D.A., Grimm, J., Lintault, L., Newman, J., Reczek, E.E., Weissleder, R., and Jacks, T. (2007). Restoration of p53 function leads to tumour regression in vivo. Nature *445*, 661–665. https://doi.org/10.1038/nature05541.
58. Knudson, C.M., Tung, K.S., Tourtellotte, W.G., Brown, G.A., and Korsmeyer, S.J. (1995). Bax-Deficient Mice with Lymphoid Hyperplasia and Male Germ Cell Death. Science *270*, 96–99. https://doi.org/10.1126/science.270.5233.96.
59. Danielian, P.S., Muccino, D., Rowitch, D.H., Michael, S.K., and McMahon, A.P. (1998). Modification of gene activity in mouse embryos in utero by a tamoxifen-inducible form of Cre recombinase. Curr. Biol. *8*, 1323–1326. https://doi.org/10.1016/s0960-9822(07)00562-3.
60. Dobin, A., Davis, C.A., Schlesinger, F., Drenkow, J., Zaleski, C., Jha, S., Batut, P., Chaisson, M., and Gingeras, T.R. (2013). STAR: Ultrafast universal RNA-seq aligner. Bioinformatics *29*, 15–21. https://doi.org/10.1093/bioinformatics/bts635.
61. Anders, S., and Huber, W. (2010). Differential expression analysis for sequence count data. Genome Biol. *11*, R106. https://doi.org/10.1186/gb-2010-11-10-r106.
62. Chu, V.T., Weber, T., Graf, R., Sommermann, T., Petsch, K., Sack, U., Volchkov, P., Rajewsky, K., and Kühn, R. (2016). Efficient generation of Rosa26 knock-in mice using CRISPR/Cas9 in C57BL/6 zygotes. BMC Biotechnol. *16*, 4. https://doi.org/10.1186/s12896-016-0234-4.
63. Kinameri, E., Inoue, T., Aruga, J., Imayoshi, I., Kageyama, R., Shimogori, T., and Moore, A.W. (2008). Prdm proto-oncogene transcription factor family expression and interaction with the Notch-Hes pathway in mouse neurogenesis. PLoS One *3*, e3859. https://doi.org/10.1371/journal.pone.0003859.
64. Joyner, A.L., and Martin, G.R. (1987). En-1 and En-2, two mouse genes with sequence homology to the Drosophila engrailed gene: expression during embryogenesis. Genes Dev. *1*, 29–38. https://doi.org/10.1101/gad.1.1.29.
65. Dong, X., Han, S., Zylka, M.J., Simon, M.I., and Anderson, D.J. (2001). A diverse family of GPCRs expressed in specific subsets of nociceptive sensory neurons. Cell *106*, 619–632. https://doi.org/10.1016/S0092-8674(01)00483-4.
66. Chen, C.L., Broom, D.C., Liu, Y., De Nooij, J.C., Li, Z., Cen, C., Samad, O.A., Jessell, T.M., Woolf, C.J., and Ma, Q. (2006). Runx1 determines nociceptive sensory neuron phenotype and is required for thermal and neuropathic pain. Neuron *49*, 365–377. https://doi.org/10.1016/j.neuron.2005.10.036.
67. Ren, A.J., Wang, K., Zhang, H., Liu, A., Ma, X., Liang, Q., Cao, D., Wood, J.N., He, D.Z., Ding, Y.Q., et al. (2014). ZBTB20 regulates nociception and pain sensation by modulating TRP channel expression in nociceptive sensory neurons. Nat. Commun. *5*, 4984. https://doi.org/10.1038/ncomms5984.
68. Cau, E., Gradwohl, G., Fode, C., and Guillemot, F. (1997). Mash1 activates a cascade of bHLH regulators in olfactory neuron progenitors. Development *124*, 1611–1621. https://doi.org/10.1242/dev.124.8.1611.

STAR★METHODS

KEY RESOURCES TABLE

REAGENT or RESOURCE	SOURCE	IDENTIFIER
Antibodies		
Rabbit polyclonal anti-GFP	Molecular Probes	Cat# A-6455; RRID:AB_221570
Rabbit polyclonal anti-H3P	Millipore	Cat# 06–570; RRID:AB_310177
Mouse monoclonal anti-Islet1	DSHB	Cat# 39.4D5; RRID:AB_2314683
Mouse monoclonal anti-Nkx6.1	DSHB	Cat.#F55A10-s; RRID:AB_532378
Rabbit polyclonal anti-P2X2	Alomone labs	Cat.# APR-003; RRID:AB_2040054
Mouse monoclonal anti-Sox10	Abcam	Cat.# ab216020; RRID:AB_2847913
Rabbit polyclonal anti-TH	Pel-Freez Biologicals	Cat.#P40101-150; RRID:AB_2617184
Mouse monoclonal anti-Brn3a	Millipore	Cat.# MAB1585; RRID:AB_94166
Chicken polyclonal anti-Peripherin	Abcam	Cat.# ab106276; RRID:AB_10863669
Rabbit polyclonal anti-DsRed	Takara Bio	Cat.# 632496; RRID:AB_10013483
Mouse monoclonal anti-GATA-3	Santa Cruz Biotechnology	Cat.# SC268; RRID:AB_2108591
Goat polyclonal anti-TrkB	R&D Systems	Cat.# AF1494; RRID:AB_2155264
Goat polyclonal anti-TrkC	R&D Systems	Cat.# AF1404: RRID:AB_2155412
Rabbit polyclonal anti-cleaved Caspase 3	Cell Signaling	Cat.# 9661; RRID:AB_2341188
Goat polyclonal anti-TrkA	R&D Systems	Cat.# AF1056; RRID:AB_2283049
Rabbit Polyclonal anti-TrkA	gift from L. Reichardt	N/A
Rabbit polyclonal anti-βTubulin III	Merck	Cat.#T2200; RRID:AB_262133
Mouse monoclonal anti-Neurofilament (NF-M)	DSHB	Cat.# 2H3; RRID:AB_531793
Chicken polyclonal anti-β-galactosidase	Abcam	Cat.# ab9361; RRID:AB_307210
Rabbit polyclonal anti-Skor2	Novus Biologicals	Cat.# NBP2-14565; RRID:AB_2632379
Rabbit Polyclonal anti-Phox2a	gift from J.-F. Brunet	N/A
Rabbit Polyclonal anti-Phox2b	gift from J.-F. Brunet	N/A
Guinea-pig polyclonal anti-Prdm12	Desiderio et al.[11]	N/A
Guinea-pig polyclonal anti-Tlx3	gift from Thomas Müller	N/A
Rabbit polyclonal anti-Tlx3	gift from Thomas Müller	N/A
Goat anti-rabbit IgG Alexa Fluor 488 conjugated	Molecular Probes	Cat.# A-11008; RRID:AB_143165
Goat anti-rabbit IgG Alexa Fluor 594 conjugated	Molecular Probes	Cat.# A-11012; RRID:AB_141359
Goat anti-rabbit IgG CF405S conjugated	Gentaur	Cat.# 20082; RRID:AB_10561326
Goat anti-mouse IgG Alexa Fluor 488 conjugated	Molecular Probes	Cat.# A-11029; RRID:AB_2534088
Goat anti-mouse IgG Alexa Fluor 594 conjugated	Molecular Probes	Cat.# A-11005; RRID:AB_141372
Goat anti-guinea pig IgG Alexa Fluor 488 conjugated	Molecular Probes	Cat.# A-11073; RRID:AB_2534117
Goat anti-guinea pig IgG Alexa Fluor 594 conjugated	Molecular Probes	Cat.# A-11076; RRID:AB_141930
Donkey anti-rabbit IgG Alexa Fluor 488 conjugated	Abcam	Cat.# ab150073; RRID:AB_ 2636877
Donkey anti-rabbit IgG Alexa Fluor 405 conjugated	Abcam	Cat.# ab175651; RRID:AB_ 2923541
Donkey anti-guinea pig IgG Alexa Fluor 488 conjugated	Jackson ImmunoResearch Labs	Cat.# 706-545-148; RRID:AB_2340472
Donkey anti-guinea pig IgG Alexa Fluor 405 conjugated	Abcam	Cat.# ab175678; RRID:AB_ 2827755
Donkey anti-goat IgG Alexa Fluor 594 conjugated	Molecular Probes	Cat.# A11058; RRID:AB_ 142540
Donkey anti-chicken IgG Alexa Fluor 488 conjugated	Jackson ImmunoResearch Labs	Cat.# 703-545-155; RRID:AB_2340375
Chemicals, peptides, and recombinant proteins		
Tamoxifen	Merck	Cat.#T5648
NeuroVue®Jade	Polyscience, Warrington, PA	Cat.# 248 37-1

(*Continued on next page*)

Continued

REAGENT or RESOURCE	SOURCE	IDENTIFIER
Critical commercial assays		
TruSeq RNA Library Preparation Kit v2	Illumina	Cat.# RS-122-2001; RS-122-2002
Deposited data		
RNA-seq Data	This manuscript	GEO: GSE211929
RNA-seq Data	Latragna et al.[39]	GEO: GSE182904
Experimental models: Organisms/strains		
Mouse: *Prdm12*^{LacZ}	Desiderio et al.[11]	N/A
Mouse: *Prdm12*^{flox}	Desiderio et al.[11]	N/A
Mouse: Rosa26$^{LSLtdTomato;}$ B6; 129S6-Gt(ROSA)26Sor$^{tm14(CAG-tdTomato)Hze/J}$	Madisen et al.[56]	JAX: 007908
Mouse: *Advillin*-Cre; B6.129P2-Avil$^{tm2(cre)Fawa/J}$	Zhou et al.[33]	JAX:032536
Mouse: *Rosa26*^{CreERT2}; B6.129 Gt(ROSA)26Sor$^{tm1(cre/ERT2)Tyj/J}$	Ventura et al.[57]	JAX:008463
Mouse: *Phox2b*^{LacZ}	Pattyn et al.[7]	N/A
Mouse: *Phox2b*-Cre	D'Autréaux et al.[4]	N/A
Mouse: *Sox10*-Venus	Shibata et al.[20]	N/A
Mouse: *Ngn1*$^{GFP/+}$:Neurog1^{tm1And}/Neurog1^{tm1And}	Ma et al.[18]	N/A
Mouse: *Dbx1*-Cre; Dbx1$^{tm2(cre)Apie}$	Bielle et al.[36]	N/A
Mouse: *Nav1.8*-Cre	Stirling et al.[43]	N/A
Mouse: *Bax*$^{-/-}$; B6.129X1-Bax$^{tm1Sjk/J}$	Knudson et al.[58]	JAX:002994
Mouse: *Wnt1*-Cre	Danielian et al.[59]	N/A
Mouse: *Rosa26*$^{LSL\text{-}Prdm12}$	This manuscript	N/A
Oligonucleotides		
Prdm12^{LacZ} – Fwd: 5′-AGTTTGTACATTCCCTGGGAGTAAGACTCC-3′	This manuscript	N/A
Prdm12^{LacZ} – Rev: 5′-AGCCAGGGGAAGAATGTGAGTTGC-3′	This manuscript	N/A
Prdm12^{flox} – Fwd: 5′-GCTGATCGAGTCCAGGAGAC-3′	This manuscript	N/A
Prdm12^{flox} – Rev: 5′-CCAAACATCCACAACCTTCA-3′	This manuscript	N/A
Cre – Fwd: 5′-CGATGCAACGAGTGATGAGGTTC-3′	This manuscript	N/A
Cre – Rev: 5′-GCACGTTCACCGGCATCAAC-3′	This manuscript	N/A
Sox10-Venus – Fwd: 5′-AAGACGTGGAGGCGGGACGC-3′	This manuscript	N/A
Sox10-Venus – Rev: 5′-CACCACCCCGGTGAACAGCTCC-3′	This manuscript	N/A
Neurog1 WT – Fwd: 5′-TGGTGTCGTCGGGGAACGAG-3′	This manuscript	N/A
Neurog1^{GFP} – Fwd: 5′-AAGGCCGACCTCCAAACCTC-3′	This manuscript	N/A
Neurog1^{GFP}/WT – Rev: 5′-CCTGTACATAACCTTCGGGC-3′	This manuscript	N/A
Rosa26^{LSLtdTomato} – Fwd: 5′-GGCATTAAAGCAGCGTATCC-3′	This manuscript	N/A
Rosa26^{LSLtdTomato} – Rev: 5′-CTGTTCCTGTACGGCATGG-3′	This manuscript	N/A
Bax WT – Fwd: 5′-GCAGAGGGTTAAAAGCAAGG-3′	JAX Protocol	JAX:002994
Bax Mutant– Fwd: 5′-CTTCCTGACTAGGGGAGGAG-3′	JAX Protocol	JAX:002994
Bax WT/Mutant– Rev: 5′-ACCCAGCCACCCTGGTCT-3′	JAX Protocol	JAX:002994
Software and algorithms		
GraphPad Prism	GraphPad	https://www.graphpad.com/
Star Alignment software 2.3.0e	Dobin et al.[60]	https://bioweb.pasteur.fr/packages/pack@STAR@2.3.0e
SAMtools 0.0.18	Li et al., 2009	http://samtools.sourceforge.net/
R/Bioconductor	Bioconductor	https://bioconductor.org/
DEseq2 1.8.2	Anders and Huber.[61]	http://bioconductor.org/

(*Continued on next page*)

Continued

REAGENT or RESOURCE	SOURCE	IDENTIFIER
Other		
Stk32a RNAscope probe	ACD Biotechne	Cat.# 509691
Agtr1a RNAscope probe	ACD Biotechne	Cat.# 481161-C3

RESOURCE AVAILABILITY

Lead contact

Further information and request for resources and reagents should be directed to and will be fulfilled by the Lead Contact, Eric Bellefroid (ebellefr@ulb.ac.be).

Materials availability

The *Rosa26*$^{LSL\text{-}Prdm12}$ mouse line generated in this study is available from the lead contact upon completion of a Material Transfer Agreement.

Data and code availability

- RNAseq raw data files have been deposited on the NCBI Gene Expression Omnibus and are publically accessible (GEO Accession viewer (nih.gov)). Accession numbers are listed in the key resources table.
- This paper does not report original code.
- All data needed to evaluate the conclusions in the paper are present in the paper and/or the Supplementary Materials.Any additional information required to reanalyze the data reported in this paper is available from the lead contact upon request.

EXPERIMENTAL MODEL AND STUDY PARTICIPANT DETAILS

Mice

All animal experiments were performed with approval from the CEBEA (Comité d'éthique et du bien-être animal) of the IBMM-ULB and conformed to the European guidelines on the ethical care and use of animals. All mice were maintained on a C57BL/6J background and 2–8 months old mice of either sex were used. Mice were housed under standard conditions and given chow and water *ad libitum*. Air circulation in the facility was filtered and temperature monitored at 20°C. Experiments were designed to minimize the number of animals used. Primers used for genotyping were indicated in the key resources table. The following mouse strains were used: *Prdm12*$^{LacZ/+}$ and *Prdm12*$^{flox/flox}$[11]; Rosa26^{LSLtdTomato} (Ai14, JAX# 007908)[56]; *Advillin*-Cre (JAX# 032536)[33];*Rosa26*^{CreERT2} (JAX# 008463)[57]; *Bax*$^{-/-}$ (JAX#002994)[58]; *Phox2b*$^{LacZ/+}$ and *Phox2b*-Cre mice.[4,7] *Sox10*-Venus,[20] *Neurog1*^{GFP},[18] *Dbx1*-Cre[36] and *Nav1.8*-Cre[43] mice were gifts from S. Shibata, François Guillemot, A. Pierani and E. Bourinet, respectively.

CRISPR Cas9-mediated knock-in into the *Rosa26* locus was used to generate the conditional Prdm12 overexpressing (*Rosa26*$^{LSL-Prdm12/+}$) mice. PR26 CAG/GFP Asc plasmid was used as conditional (Cre/*loxP*) targeting vector (addgene #74285). Mouse Prdm12 coding sequence was amplified by PCR and was cloned into the targeting vector using the AscI cloning site. sgRNA26-1[62] was used as guide RNA to create double-strand break at the Rosa26 intronic XbaI site. The guide RNA is split in two parts: 1) crRNA (20 nucleotides), corresponding to the target sequence (protospacer) with a tail (16 nucleotides) and 2) tracrRNA (67 nucleotides), containing the hairpin recognized by Cas9 with an extremity complementary to the crRNA tail. Annealed crRNA/tracrRNA (2.4 pmol/μL), Cas9 nuclease V3 (200 ng/μL) and Prdm12 targeting vector (10 ng/μL) were mixed in IDTE buffer and injected into the pronucleus of B6D2F2 mouse zygotes. Injected zygotes were incubated in KSOM medium at 37°C for at least 2 h before being transferred into oviduct of CD1 pseudo-pregnant female mice. Identification of positive founders with correct targeting was done by PCR genotyping and confirmed by sequencing. crRNA, tracrRNA (1072534), Cas9 nuclease V3 (1081059) and IDTE (11-01-02-02) were ordered from Integrated DNA Technology (IDT).

METHOD DETAILS

Embryo processing

In situ hybridizations and immunofluorescence stainings were performed on cryostat sections as previously described.[11,37] Detailed methods and antisense probes and antibodies used can be found in SI Appendix, supplemental materials and methods. Quantitative analyses were carried out on at least 3 independent animals of each genotype. Statistical analysis was performed using the GraphPad Prism software.

Tamoxifen treatment

Tamoxifen (Merck) was dissolved in corn oil and administrated intraperitoneally (1.9 mg/25g body weight) in more than 56- day-old 4 times in a week for the *Rosa26*^{CreERT2}; *Prdm12*^{flox} mice. Injected animals were killed 28 to 35 days after the last Tamoxifen injection for analysis.

In situ hybridizations and immunostainings

For *in situ* hybridization, embryos or, if older than E12.5 head and body parts, were dissected in cold RNase-Free (RF) PBS 1X, fixed over-night (O/N) in 4% PFA (diluted in RF-PBS) at 4°C, and cryoprotected by incubation in sucrose 30% (diluted in RF-PBS) until tissue sank. Fixed infused tissues were then embedded in gelatin 7,5% - sucrose 15% (diluted in RF-PBS) and stored at −80°C before cryostat sectioning (20 μm). *In situ* hybridization were performed as previously described.[37] Antisense RNA probes were synthetized using the MEGAscript T7/T3 or SP6 kit (ThermoFisher) following the manufacturer's instructions and labeled using the digoxigenin-11-UTP (Roche). Images collection and analysis were performed using a stereo microscope Olympus SZX16 and the software CellSens Entry V2.1 or Zeiss Axio Observer Z1. using the ZENblue software.

Plasmids used to generate antisense probe for mouse *Prdm12*,[63] *Engrailed-1*,[64] *Evx1*,[11] *Dbx1*,[36] *Neurog1*,[18] *Ntrk1*,[17] *Ret*,[65] *Runx1*,[66] *Scn10a*,[67] *NeuroD1*,[68] *Pou4f1*,[16] *DBH*[49] have been described previously. EST Horizon clone Id:30431573 was used to generate the *Slc6a2* antisense probe.

For immunofluorescence staining, embryos were dissected in cold PBS 1X, fixed 20 min in 4% PFA at 4°C, then cryoprotected by incubation in sucrose 30%. Embryos were then embedded in gelatin 7,5% - sucrose 15% and stored at −80°C. After freezing, embryos were cryosectioned at 14-18 μm. For the staining procedure, all sections were dried 20 min at RT, rinsed 3 × 10 min with PBS, blocked with 10% normal serum (donkey or goat) in 0.1% PBST (0.1% Triton X-100 in PBS) for 2 h, and incubated with primary antibody(ies) in blocking solution overnight at 4°C. The following day, sections were rinsed 3 × 10 min with PBST and incubated with secondary antibodies 1 h at RT with secondary antibody(ies) diluted in the same buffer. Sections were then rinsed 3 × 10 min in PBST, counterstained with DAPI and/or rinsed 2 × 5 minutes in PBS and mounted under coverslips in Dako fluorescence mounting medium (DAKO cat.#S3023) and rapidly imaged. Primary and secondary antibodies used in this study were listed in the key resources table. Antigen retrieval, by boiling for 10 min in sodium citrate (10 mM), was needed for optimal labeling with anti-Islet and anti-Brn3a antibodies. Images collection and analysis were performed using a wide-field fluorescence microscope Zeiss Axio Observer Z1 or a laser-scanning confocal microscope Zeiss LSM 710 using the Zeiss Zen microscopy software.

NeuroVueJade retro labeling

For NeuroVueJade retro labeling (Polyscience, Warrington, PA), embryos head were first dissected in cold PBS 1X, fixed 20 min in 4% PFA at 4°C, and then left in 1% PFA for several days at 4°C. On the day of the labeling, the head of the embryos were immobilized by inserting a needle into the tong and the neck and small incisions with forceps were made in the middle of the whisker pads in order to facilitate the insertion of small triangle pieces of NeuroVueJade (green emitting dye; excitation maximum, 478 nm; emission maximum, 508 nm). The heads are then rapidly put back in 1% PFA and left for incubation in the dark at RT for around three weeks. The NeuroVueJade signal progression in the tissue was regularly checked using a binocular with fluorescent lamp. Once the signal reached nerves at the level of the eyes, heads were post-fixed in 4% PFA – 0,25% glutaraldehyde on ice for 20 min, then quickly washed in cold PBS 1X and incubated in sucrose 30% at 4°C in the dark until tissue sank. Embryos heads were embedded in gelatin 7,5% - sucrose 15% and stored at −80°C before cryostat sectioning. IF experiments were next performed on 25 μm parasagittal sections with a modified protocol,[32] that uses digitonin (stock at 50 mg/mL dissolve in DMSO) which is a more compatible detergent for co-staining with lipophilic dyes than Triton X100. Briefly, the sections were washed in PBS 1X, then incubated 1 h at RT in blocking solution (10% serum and digitonin 1/50 in PBS 1X). Primary and secondary antibodies were diluted in blocking solution, and all washes of the second day of experiment were done with PBS 1X. After DAPI staining and PBS washes, sections were mounted in DAKO fluorescence mounting medium (DAKO cat.#S3023) and analyzed with a laser-scanning confocal microscope Zeiss LSM 710.

RNAscope

For sample preparation, individual DRG from mice were rapidly dissected in cold RF PBS 1X. DRG were embedded in OCT medium (VWR cat.# 361603E), frozen in dry-ice and stored at −80°C until they were sectioned. DRG were sectioned at a thickness of 15–20 μm and RNAs were detected by RNAscope (Advanced Cell Diagnostics) using the manufacturer's protocol. The following probes were used: *Stk32a* (ACD Biotechne cat.# 509691) and *Agtr1a* (ACD Biotechne cat.# 481161-C3).

X-gal staining on embryo sections

Embryos 20 μm sections were fixed in 4% PFA for 30 min at RT. After three washes of 30 min at RT in "detergent rinse" solution (2 mM MgCl2, 0.01% sodium deoxycholate, 0.02% NP-40 diluted in PBS 1X), the sections were then incubated in the dark at 37°C in staining solution composed of detergent rinse solution with 5 mM K3Fe(CN)6, 5 mM K4Fe(CN)6 and 1 mg/ml of X-gal. When X-gal staining was sufficient, sections were rinsed several times in PBS 1X, post-fixed in 4% PFA for 20 min at RT and rinsed several times in PBS 1X before mounting in DAKO fluorescence medium (DAKO cat.#S3023).

RNA sequencing and data processing

Trigeminal ganglia were dissected in cold RF PBS 1X and store at −80°C in TRIZOL (ThermoFisher cat.# 15596026). For TG isolation, E13.5 control and *Prdm12* KO embryos with a Sox10-Venus background were used to facilitate dissection. RNA was extracted using the illustra RNAspin Mini RNA isolation kit (GE Healthcare cat.# 25-0500-70). Quality and integrity of RNA was assessed with the Fragment Analyzer from Advanced Analytical by using the standard sensitivity RNA Analysis Kit (DNF-471). RNA-seq libraries were performed using 100 ng total

RNA of a nonstranded RNA Seq, massively parallel mRNA sequencing approach from Illumina (TruSeq RNA Library Preparation Kit v2, Set A; 48 samples, 12 indexes, Cat. NRS-122-2001). Libraries were prepared on the automation (Beckman Coulter's Biomek FXP workstation). For accurate quantitation of cDNA libraries, a fluorometric-based system, the QuantiFluordsDNA System from Promega (Madison, WI) was used. The size of final cDNA libraries was determined by using the dsDNA 905 Reagent Kit (Fragment Analyzer from Advanced Bioanalytical) exhibiting a sizing of 280 bp in average. Libraries were pooled and sequenced on the Illumina HiSeq 4000 (SE; 50 bp; 30 Mio reads/sample). Sequence images were transformed to BCL files with the Illumina software BaseCaller software, which were demultiplexed to fastq files using bcl2fastq v2.20.0.422. Sequencing quality was asserted using FastQC software (http://www.bioinformatics.babraham.ac.uk/projects/fastqc/)(version 0.11.5). Sequences were aligned to the Mus musculus GRCm39 genome using the STAR aligner software version 2.7.8a,16 allowing for 2 mismatches within 50 bases. Subsequently, read counting was performed using feature-eCounts version 2.0.1.34 Read counts were analyzed in the R/Bioconductor environment version 4.1.0 (www.bioconductor.org) using the DESeq2 package version 1.32.0.37 Candidate genes were selected as those with an FDR-corrected P-value #0.05. Genes were annotated using the M musculus GTF file mm10 version 104 used to quantify the reads within genes.

Analysis of cell type attribution to the identified dysregulated genes in E13.5 *Prdm12*$^{LacZ/LacZ}$ TG was performed using the gene expression atlases developed by Usoskin et al. 2015[23] (linnarssonlab.org/drg/), Zeisel et al. 2018[24] (mousebrain.org) and Kupari et al. 2019[26] (https://ernforsgroup.shinyapps.io/vagalsensoryneurons/). Dysregulated genes were categorized as ''Neuron enriched'' if they had significant expression in at least in one neuronal cell type (and no or limited expression in non-neuronal cell types), in at least one of the used gene expression visualization tools. RNA-seq data have been deposited at Gene Expression Omnibus (GEO) under accession GSE211929.

QUANTIFICATION AND STATISTICAL ANALYSIS

Quantitative analyses were carried out on at least 3 independent animals of each genotype. All statistical analyses and the generation of graphs were performed using the GraphPad software.

Statistical tests used are specified in the legends of the figures and supplementary figures wherever appropriate. In cases in which our datasets did not follow normal distribution, nonparametric statistical tests have been applied. In cases in which our datasets do not contain enough biological replicates to be able to determine whether they follow a normal distribution or not, non-parametric tests have been also applied. No statistical methods have been used to determine sample sizes.